

A flow equation approach to periodically driven quantum systems

Michael Vogl*, Pontus Laurell*, Aaron D. Barr, and Gregory A. Fiete
Department of Physics, The University of Texas at Austin, Austin, TX 78712, USA
(Dated: August 4, 2022)

We present a theoretical method to generate a highly accurate *time-independent* Hamiltonian governing the finite-time behavior of a time-periodic system. The method exploits infinitesimal unitary transformation steps, from which renormalization group-like flow equations are derived to produce the effective Hamiltonian. Our tractable method has a range of validity reaching into frequency regimes that are usually inaccessible via high frequency ω expansions in the parameter \hbar/ω , where \hbar is the upper limit for the strength of local interactions. We demonstrate our approach on both interacting and non-interacting many-body Hamiltonians where it offers an improvement over the more well-known Magnus expansion and other high frequency expansions. For the interacting models, we compare our approximate results to those found via exact diagonalization. While the approximation generally performs better globally than other high frequency approximations, the improvement is especially pronounced in the regime of lower frequencies and strong external driving. This regime is of special interest because of its proximity to the resonant regime where the effect of a periodic drive is the most dramatic. Our results open a new route towards identifying novel non-equilibrium regimes and behaviors in driven quantum many-particle systems.

I. INTRODUCTION

Recent years have seen rapid progress in our understanding of dynamics and non-equilibrium phenomena in quantum systems [1, 2]. This has been a result of experimental advances in the ability to control cold atom [2–4] and condensed matter systems [5–7], by developments in time-resolved laser techniques [8, 9], and by the fact that stepping into the time domain opens up new ways of ultrafast control of material properties [5, 10, 11] and access to different phases of matter. These include photoinduced superconductivity [12, 13], hidden orders [14], and metastable states [15], but also entirely novel phases, such as time crystals [16, 17] and non-equilibrium topological phases [18, 19].

In particular, there has been growing interest in periodically driven (or Floquet) [20, 21] many-body systems, which can bear a close resemblance to equilibrium systems [22]. The Floquet systems come in three established thermodynamic classes: integrable [23, 24], many-body localized (MBL) [19, 25, 26], and generic interacting ones [27]. The first two classes can avoid thermalization, allowing for a notion of a Floquet phase of matter at long stroboscopic times $t = nT$, where T is the period of the Hamiltonian, $H(t + T) = H(t)$, and n is an integer. The physics of these phases is captured by an effective, time-independent Floquet Hamiltonian H_F , given via the time evolution operator over one period $U(T) = \exp(-iH_F T)$.

In non-interacting systems H_F can be used to dynamically engineer interesting and topological band structures [28–37], most notably Floquet topological insulators [38–43]. Our main interest, however, is interacting systems where H_F can be engineered to drive phase transitions

[44, 45], or, in the case of Floquet-MBL systems, realize new phases without equilibrium analogs [18, 19, 46, 47]. Clean interacting Floquet systems are the least studied of the three classes, perhaps because they were expected to heat up to a featureless state with infinite effective temperature [48, 49]. However, it was recently theoretically discovered that under very general conditions they may remain in a prethermal state until exponentially long times τ^* [50–54], which has been verified numerically in several models [55, 56].

The existence of a prethermal regime is important because realistic systems usually contain integrability-breaking perturbations that support it, and because the thermalization time τ^* can correspond to experimentally accessible time scales. The existence of such a regime also implies that there is interesting physics to be found at intermediate times $0 < t < \tau^*$ [50, 57], where one may use time-dependent perturbations to drive dynamical phase transitions [58–61], control interactions [62, 63], or engineer phase transitions and topological phases [64–68].

To understand the properties of a system in the prethermal regime, it is convenient to use a description in terms of the effective Hamiltonian, H_F . It is, however, notoriously difficult to calculate H_F or the exact time-evolution operator $U(t)$ for interacting systems, so generally one uses an expansion technique to find an approximate, effective Hamiltonian in the high-frequency limit. These include the Magnus expansion [69–71], rotating frames [51], and many more [20, 65, 72–78]. Unfortunately, these methods do not produce cleanly convergent expansion series for general systems. Instead, they are asymptotic expansions, subject to an optimal cut-off order which prevents them from, even in principle, reaching into the lower frequency regimes [51, 69].

One of the more controlled descriptions of a system occurs in the quasiequilibrium regime, $W \ll \hbar\omega \ll \Delta$, where W is the bandwidth of the system, ω the driving frequency, and Δ is the gap to the continuum of

*These authors contributed equally to this work.

higher energy states. While this separation of energy scales is quite feasible in cold atom systems, it is harder to reach in solid state systems. Mott insulators are the most promising class of systems in this regard, but even there the range of frequencies is limited since we typically have $W \sim 1\text{eV}$ and $\Delta \sim 1\text{eV}$, which are of the same order of magnitude. In addition, lower frequency regimes are required for certain topological phases [18], and are of interest also in cold atom systems [79, 80]. Hence, techniques to handle lower frequencies are needed.

In this paper we improve on the limitations of previous methods, and provide better access to lower frequencies and higher driving strengths. To achieve this we introduce a formalism to remove the time-dependent part of a Hamiltonian using infinitesimal unitary transformations. This results in flow equations for different couplings, reminiscent of renormalization group calculations [81] and Wegner's flow-equation approach to diagonalizing Hamiltonians [82, 83]. There has also recently been progress in using the Wegner flow to describe the time-evolution of a many-body localized system [84], which however still requires the solution of flow equations for each time-step - a problem we avoid in our construction. We describe both the exact flow equations, and ways to approximate them. We apply our method to four spin chain Hamiltonians: (i) an integrable XY model with antisymmetric exchange, (ii, iii) two integrability breaking extensions of a J_1 - J_2 -type XXZ model [85], and (iv) the transverse field Ising model.

The extended XY model is driven by a transverse magnetic field, the first J_1 - J_2 -type XXZ model is driven locally by a x -direction magnetic field, and the second by a nearest neighbor Ising exchange interaction, making for a time-dependent J_1 - J_2 model [86, 87]. For the transverse field Ising model we consider a case where the time evolution operator factorizes into two matrix exponentials which allows us to find a family of different resummations of the Baker-Campbell-Hausdorff (BCH) identity and leaves open the question as to how to construct the optimal effective Hamiltonian for a given time evolution operator (reverse of the usual situation in which one seeks the optimal time evolution operator approximation for a given Hamiltonian).

We study the time evolution of the exact models, and their effective models obtained in our approach. We compare our results with those obtained by the Magnus expansion. The integrability breaking models are studied numerically using full exact diagonalization, which provides an unbiased test of the validity of our approach. We find that our flow method generally outperforms the Magnus expansion, with significantly greater accuracy as the resonant regime is approached, as well as in the case when the time-dependent term in the Hamiltonian is large. Both of these cases are of direct physical relevance and interest. Our method thus opens new possibilities in the analytical and numerical simulation of time-dependent quantum many-particle systems, and will facilitate the search for novel prethermal and non-

equilibrium regimes.

Our paper is organized as follows. In Sec.II we develop the general flow-equation formalism, and discuss its implications and approximations. We relate the general results obtained from the flow equation approach to various high-frequency expansions used in the literature. In Sec.III we introduce the four different one-dimensional spin chain Hamiltonians we will use to assess the performance of this approximate method. In Sec.IV we summarize our results for the different models. In Sec.V we compare our results to a resummation of the Baker-Campbell-Hausdorff identity that was of recent interest [88], and in Sec.VI we present our main conclusions. Various technical details and formulas appear in the appendices.

II. GENERAL FORMALISM

We take the Schrödinger equation of a periodically driven many-particle system as our starting point. Following Ref. [51], the Hamiltonian $H(t)$ is split into a constant part $H_0 = \frac{1}{T} \int_0^T dt H(t)$, and a time-periodic term $V(t) = \frac{1}{T} \int_0^T dt_1 (H(t) - H(t_1))$ that averages to zero over one period, $\frac{1}{T} \int_0^T dt V(t) = 0$. Thus, the time-dependent Schrödinger equation takes the form,

$$i\partial_t |\psi_0\rangle = (H_0 + V(t)) |\psi_0\rangle, \quad (1)$$

where we have set Planck's reduced constant $\hbar = 1$.

We introduce a unitary transformation, $U = e^{\delta\Omega(t)}$, generated by an as yet undetermined quantity $\delta\Omega$ that will be chosen to reduce the time-dependent term $V(t)$. The δ in front of the Ω indicates we keep the generator infinitesimal, which ensures that the exponential can be safely expanded to lowest order.

Let us now introduce a new wavefunction $|\phi_{\delta s}\rangle = U^\dagger |\psi_0\rangle = [1 - \delta\Omega(t)] |\psi_0\rangle$ and act with $U(t)^\dagger = 1 - \delta\Omega(t)$ from the left on the Schrödinger equation. This new wavefunction now fulfills the modified Schrödinger equation (keeping lowest order in $\delta\Omega$ only),

$$i\partial_t |\phi_{\delta s}\rangle = (H(t) - i\partial_t \delta\Omega(t) - [\delta\Omega(t), H(t)]) |\phi_{\delta s}\rangle. \quad (2)$$

One may read off a new Hamiltonian, which, since $\delta\Omega$ is infinitesimal, can be written as

$$\tilde{H}(t) = H(t) - i\partial_t \delta\Omega(t) - [\delta\Omega(t), H(t)]. \quad (3)$$

We now choose $\delta\Omega$ such that it reduces the time dependent part of the Hamiltonian $V(t) \rightarrow (1 - \delta s)V(t)$ by some infinitesimal value δs ,

$$\delta\Omega = -\frac{i}{T} \delta s \int_0^t dt_1 \int_0^T dt_2 (H(t_1) - H(t_2)), \quad (4)$$

which also leaves a residual time dependence of $\delta s [V(t), H(t)]$ in Eq.(3), which is small in magnitude if δs is small.

This generator in Eq.(4) also has the nice property that it vanishes at stroboscopic times T . Therefore, at stroboscopic times, expectation values $\langle O \rangle$ of operators O can be calculated without a change of basis. The behavior at other times can be found by applying the unitary transformation to the operator O .

One could now repeat the procedure of splitting the Hamiltonian into a constant and a time average zero part and then apply this infinitesimal unitary transformation to find the Floquet Hamiltonian after an infinite amount of steps (or an approximation to it by stopping after a finite amount of steps). To simplify the process, we recognize that one can track the progress of the unitary transformations by a single flow parameter, s . To do so we extend the functional dependencies of the Hamiltonian to include this parameter, replacing $H(t) \rightarrow H(s, t)$ and $\tilde{H}(t) \rightarrow H(s + \delta s, t)$. Note that $H(s, t)$ represents a family of effective Hamiltonians interpolating between a starting Hamiltonian $H(0, t)$, and the Floquet Hamiltonian $H(\infty, t)$. We also set appropriate boundary conditions by enforcing that $s = 0$ correspond to the initial, non-transformed Hamiltonian. With this notation, Eq. (3) takes the form

$$H(s + \delta s, t) = H(s, t) - \delta s V(s, t) + i \delta s \int_0^t dt_1 [V(s, t_1), H(s, t)], \quad (5)$$

with $V(s, t) = \frac{1}{T} \int_0^T dt_1 (H(s, t) - H(s, t_1))$.

Taylor expanding the left hand side since δs is infinitesimal we find,

$$\frac{dH(s, t)}{ds} = -V(s, t) + i \int_0^t dt_1 [V(s, t_1), H(s, t)], \quad (6)$$

which is a central result of this work. We refer to Eq.(6) as the exact flow equation. This equation is similar in spirit to the infinitesimal unitary transforms that Wegner [82] employs to diagonalize an interacting Hamiltonian in the equilibrium case.

How should we interpret the flow of s in Eq. (6)? Note that $H(s, t)$ is a Hamiltonian and therefore a linear sum of the various energy contributions, and can be expressed as a sum of linear operators with coefficients $c_i(s, t)$, $H(s, t) = \sum_i c_i(s, t) \hat{O}_i$ (similar in spirit to a Landau-Ginzburg energy functional). This mathematical structure in turn also implies that $-V(s, t) + i \int_0^t dt_1 [V(s, t_1), H(s, t)] = -\sum_i g_i[\{c_j(s, t' \in [0, T])\}] \hat{O}_i$, where g_i has a functional dependence on the $c_j(s, t)$ because $V(s, t)$ itself depends on the $c_j(s, t)$ and it appears under an integral.

One may therefore write Eq. (6) as

$$\frac{dc_i(s, t)}{ds} = -g_i[\{c_j(s, t' \in [0, T])\}], \quad (7)$$

which is just a flow equation for the coupling parameters $c_i(s, t)$ at different times. The operators \hat{O}_i are generated from the kinetic and potential energy terms

of the original Hamiltonian, Eq.(1), as the Hamiltonian flows. In general, new terms are generated such as hopping and interaction terms that involve more and more sites of a lattice as the order of the transformation increases. These new terms can in principle change the balance of kinetic and potential energy in the effective time-independent Hamiltonian and therefore may lead to new physical regimes for a periodically driven many-particle quantum system.

Eq.(6) offers a convenient starting point to approximate the Floquet Hamiltonian. In particular, it allows us to improve on the various high frequency expansions of the Floquet Hamiltonian that have appeared in the literature. We can find an analytically tractable equation if we set $s = 0$ only for the terms $V(s, t)$. This corresponds to removing the original time dependent part $V(t)$ from the Hamiltonian via the transformation $e^{-i \int_0^t dt V(t)}$, while generating other new time dependences. To ensure that it actually corresponds to the aforementioned unitary transformation we also need to restrict the range of s to $[0, 1]$, rather than the previous $[0, \infty)$.

Under these assumptions Eq. (6) simplifies to

$$\frac{dH(s, t)}{ds} = -V(0, t) + i \int_0^t dt_1 [V(0, t_1), H(s, t)], \quad (8)$$

and Eq. (7) becomes

$$\frac{dc_i(s, t)}{ds} = -g_i(\{c_j(s, t)\}), \quad (9)$$

where we can write $g_i(\{c_j(s, t)\}) = \sum_j \gamma_{ji}(t) c_i(s, t)$ as a linear combination of couplings $c_i(s, t)$. We are left with a first order linear differential equation that doesn't couple coefficients c_i at different times. Gone is the more complicated structure of a functional in the c_i . The effective time-independent Hamiltonian is then given by

$$H_{\text{eff}} = \sum_i \bar{c}_i \hat{O}_i, \quad (10)$$

with $\bar{c}_i = \frac{1}{T} \int_0^T dt c_i(1, t)$, where we took an average over one period. This approximation does not make any implicit assumptions, such as $V(t)$ is small. By contrast, many other high frequency approximations do make the assumption of smallness. As a result, our approach works especially well in the limit of strong $V(t)$. We will demonstrate this explicitly in later sections of this work.

We would also like to stress that Eq. (8) implements a unitary transformation *exactly*. Its solution therefore still retains the full information of the original Hamiltonian, which means one can iterate the procedure without having to fear an optimal cut-off for the iterations. In this paper we will be content with discussing results from the first order iteration only.

Let us explicitly relate this approximation to more common high frequency approximations. For the moment, neglect $\int_0^t dt_1 [V(0, t_1), H(s, t)]$, which assumes

that all couplings in the Hamiltonian are negligible compared to the driving frequency. This is an approximation common to many of the high frequency approximations. We then find that

$$H(s, t) \approx H(0, t) - sV(t). \quad (11)$$

Inserting this back into Eq. (8) and taking a time average we find

$$H(1, t) \approx H_0 + \frac{i}{T} \int_0^T dt \int_0^t dt_1 \left[V(t_1), H_0 + \frac{1}{2}V(t) \right], \quad (12)$$

which is the lowest order of many common high frequency approximations. Hence, our approximation agrees with other approximations in the high frequency limit.

Next, we turn to an application of our method to a number of different Hamiltonians and compare our results with other approaches. We find our method nearly always provides more accurate evolution than other approximations, and in many cases our method works substantially better, particularly as the strong coupling resonant regime is approached.

III. EXAMPLE MODELS

To demonstrate the power and validity of the flow equation approach we will consider a selection of quantum spin chain ($S = \frac{1}{2}$) models. Recall that the spin operators $S_i^{x,y,z}$ fulfill the commutation relations,

$$[S_m^j, S_n^k] = i\epsilon_{jkl}\delta_{mn}S_m^l, \quad (13)$$

($j, k, l \in \{x, y, z\}$) with the special condition for $S = \frac{1}{2}$ that

$$(S_i^j)^2 = \frac{1}{4}\mathbb{1}_{\mathcal{H}}, \quad (14)$$

where $\mathbb{1}_{\mathcal{H}}$ is the unit operator in the many-body Hilbert space. Here ϵ_{jkl} is the fully antisymmetric tensor and δ_{mn} is the Kronecker delta function.

In this section we introduce four different spin models that exhibit different functional dependences of the time-dependent term. The first model (XY spin chain) is integrable, and in particular one-particle reducible. The next two models are integrability-breaking modifications to the XXZ spin chain, and the final model is a transverse field Ising model discussed independently in Sec.V. These models possess a range of different symmetries and will illustrate the generality and mathematical structure of the flow equation approach.

A. XY spin chain with antisymmetric exchange in a driven magnetic field

As a first example model we choose a XY spin-chain with an antisymmetric Dzyaloshinskii-Moriya exchange

interaction and a time-periodic magnetic field that both point along the z axis

$$H(t) = H_0 + V(t), \quad (15)$$

where

$$H_0 = \sum_i (J_x S_i^x S_{i+1}^x + J_y S_i^y S_{i+1}^y + D(\vec{S}_i \times \vec{S}_{i+1})_z + h_0 S_i^z), \quad (16)$$

and

$$V(t) = h \sin(\omega t) \sum_i S_i^z. \quad (17)$$

Here, $J_{x/y}$ is the strength of the exchange interaction in the x/y -direction, D the strength of the antisymmetric exchange, h_0 the static magnetic field strength, and h the strength of the magnetic field driving. This model has the advantage that its instantaneous Hamiltonian can be diagonalized by applying a Jordan-Wigner transformation, followed by a Bogoliubov transformation [85]. Furthermore, it has multiple coefficients, which can be varied to check the validity of our approximation based on the flow equations in a variety of cases.

B. J_1 - J_2 -model with a driven magnetic field in the isotropic plane

It is important to go beyond non-interacting models to find out if a new approximation scheme is valuable for more realistic interacting systems, so we study the J_1 - J_2 -model [86, 87],

$$H(t) = H_0 + V(t), \quad (18)$$

where

$$H_0 = \sum_{n=1}^2 \sum_i (J_n \mathbf{S}_i^\perp \mathbf{S}_{i+n}^\perp + J_n^z S_i^z S_{i+n}^z), \quad (19)$$

and

$$V(t) = \sum_i h(t) S_i^x, \quad (20)$$

with a time periodic magnetic field in the x -direction

$$h(t) = B \cdot \begin{cases} 1; & 2n\pi < \omega t < 2n\pi + \pi \\ -1; & 2n\pi + \pi < \omega t < 2(n+1)\pi \end{cases} \quad ; \quad n \in \mathbb{Z}, \quad (21)$$

where the time dependence was chosen to simplify the numerical treatment. It should be noted that J_n is the strength of the n -th neighbor exchange interaction in the isotropic plane and J_n^z is the exchange interaction in z -direction. For a more compact notation we defined $\mathbf{S}_i^\perp = (S_i^x, S_i^y, 0)$. We chose this model because the external magnetic field breaks magnetization conservation and it therefore also allows us to see if the flow equation approach works under circumstances where the driving breaks a symmetry.

C. J_1 - J_2 -model with time-dependent exchange terms

Lastly, we applied the flow equation approach to a model in which one of the spin-spin interaction terms is time-dependent. The model we consider is another J_1 - J_2 model given by,

$$H(t) = H_0 + V(t), \quad (22)$$

where

$$H_0 = \sum_i [J_1 \mathbf{S}_i^\perp \cdot \mathbf{S}_{i+1}^\perp + J_1^z S_i^z S_{i+1}^z + J_2 \mathbf{S}_i \mathbf{S}_{i+2}], \quad (23)$$

and

$$V(t) = J_{1,0}^z \text{sign} \left(\frac{\pi}{\omega} - t \cdot \text{mod}(2\pi/\omega) \right) \sum_i S_i^z S_{i+1}^z, \quad (24)$$

where mod denotes modulo. In this model, the time-dependence is in an interaction term.

IV. RESULTS

In this section we study how well our flow equation approach performs compared to common high frequency approximations. We compare the approximate time evolution operators obtained through various approximations to the exact time evolution operator at stroboscopic times.

We adhere to the following procedure: We first make use of translational invariance and calculate the exact time evolution operator $U_{ex}^k(T)$ and the approximate time evolution operator $U_{approx}^k(T)$ at different points in k -space (momentum space). Then, we calculate the mismatch of the approximate time evolution operator and the exact time evolution operator via

$$E = \frac{1}{2N\sqrt{D}} \sum_k \|U_{ex}^k(T) - U_{approx}^k(T)\|_{\text{Frob}}, \quad (25)$$

which is a quantity that takes values on the interval $[0, 1]$ with zero meaning perfect agreement and one meaning the largest possible disagreement. Here, D is the dimensionality of the Hilbert space for any given k -point, N is the number of k -points that the sum runs over, and $\|A\|_{\text{Frob}} := \sqrt{\text{tr}AA^\dagger}$ is the Frobenius norm.

Let us motivate this quantity: For a point in k -space this is just the l_2 distance of two unitary operators at this point in k -space divided by the maximum l_2 distance of two unitary operators. We average this quantity over all points of k -space. The Frobenius norm provides us with a basis-independent measure of how accurate unitary evolution of a quantum system will be with various time-independent approximations to the full time-dependent Hamiltonian. Similar formulas are used in the context of quantum information science.

A. XY Spin chain with anti-symmetric exchange

Both the Magnus expansion [see Appendix A] and the approximation via flow equations yield an effective Hamiltonian of the form,

$$H_{\text{eff}} = \sum_i (J_x^{(a)} S_i^x S_{i+1}^x + J_y^{(a)} S_i^y S_{i+1}^y + D_+^{(a)} S_i^x S_{i+1}^y + D_-^{(a)} S_i^y S_{i+1}^x + h_0 S_i^z), \quad (26)$$

where a labels the approximation scheme, with different coupling constants for different approximation schemes. The details of the derivation are given in Appendix A 1.

There are newly generated terms in Eq.(26) compared to Eq.(16). We note that a suitably chosen rotation in spin space gives back the original undriven Hamiltonian with $\Delta J = J_x - J_y$ modified.

The coupling constants for the leading order Magnus expansion are

$$J_{x,y}^{(M)} = J_{x,y}, \quad D_{\pm}^{(M)} = \pm D - \frac{(J_x - J_y)h}{\omega}, \quad (27)$$

and the results for the flow equation approach are

$$J_x^{(F)} = \frac{J_x + J_y}{2} + \frac{J_x - J_y}{2} \cos\left(\frac{2h}{\omega}\right) J_0\left(\frac{2h}{\omega}\right), \quad (28)$$

$$J_y^{(F)} = \frac{J_x + J_y}{2} - \frac{J_x - J_y}{2} \cos\left(\frac{2h}{\omega}\right) J_0\left(\frac{2h}{\omega}\right), \quad (29)$$

$$D_{\pm}^{(F)} = \pm D - \frac{J_x - J_y}{2} \sin\left(\frac{2h}{\omega}\right) J_0\left(\frac{2h}{\omega}\right). \quad (30)$$

It should be emphasized that both approximations agree in the limit of $\omega \rightarrow \infty$ — a general result mentioned previously in the end of Sec.II. We also stress that, in the case that h is much larger than all other coefficients, the flow equation approximation works well even when expanded around $2h/\omega \gg 1$, which is not what one would normally expect from a high frequency expansion. The flow equation approach does not make the assumption at any point that $V(t)$ is small, and therefore it handles this regime more accurately.

We are particularly interested in quantum many-particle systems with a large number of degrees of freedom. We therefore compute the mismatch E , Eq.(25), of time evolution operators for a long spin chain. We plot the relative error E as a function of the number of k -points to find out how many k -points are needed for a stable result. (The details on how the time evolution operator was calculated are given in Appendix B.) The plot for the Magnus expansion and for the flow equation approach are given in Fig.1.

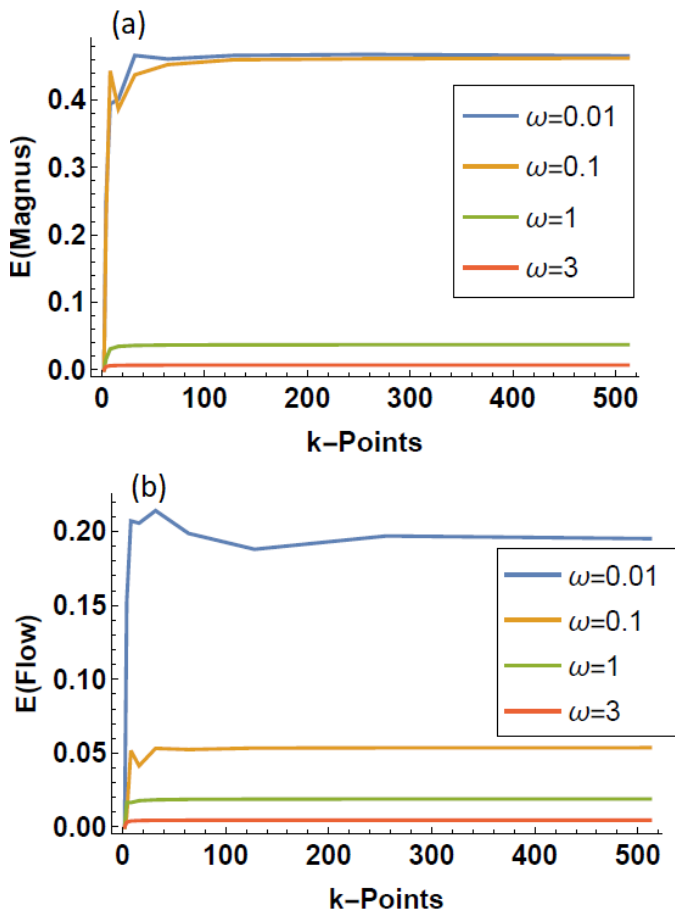


FIG. 1: (Color online.) Relative error, Eq.(25), of the time evolution operator as a function of sampled k -points for the (a) Magnus expansion and (b) Flow equation approach. Different driving frequencies $\omega = 0.01$, $\omega = 0.1$, $\omega = 1$ and $\omega = 3$ are considered. Note that the flow equation error is much smaller than the Magnus expansion error, particularly at the lowest frequencies. In both approximations, the error decreases as the frequency increases. We consider the case of $D = 0.1$, $J_x = 1$, $J_y = 1.1$, $h_0 = 1$ and $h = 1$

From Fig. 1 one can see that at 256 k-points the value of relative error E has stabilized. Therefore, for this model all further plots will be done sampling 256 k-points.

To study the accuracy of the different approximations as a function of frequency, we choose a set of coefficients $D = 0.1$, $J_x = 1$, $J_y = 1.1$, $h_0 = 1$, and $h = 1$, where J_x was fixed at unity because one may divide the Hamiltonian by J_x to make it dimensionless. The strength of D was chosen to be small since often the anti-symmetric exchange is negligible when compared to the exchange interactions. The other values were chosen to be in a similar range. The plot of the relative error E as a function of frequency ω is given in Fig. 2.

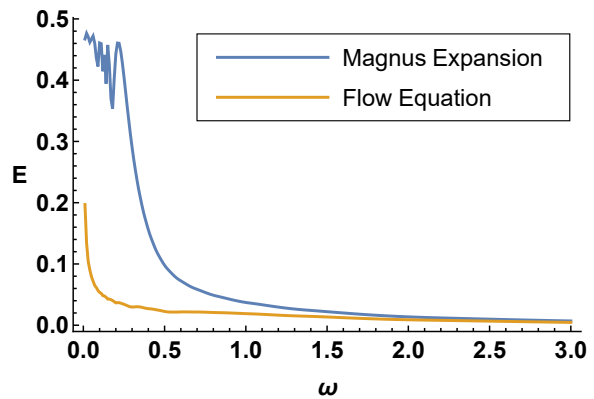


FIG. 2: (Color online.) Relative error E , Eq.(25), for $D = 0.1$, $J_x = 1$, $J_y = 1.1$, $h_0 = 1$ and $h = 1$ as a function of driving frequency ω . Note how the flow equation approach outperforms the Magnus expansion, particularly at smaller ω .

From Fig. 2 one can see that the results from the flow equation approach are valid down to much lower frequencies ω . In fact, one can expect higher order Magnus expansions to become worse at lower frequencies than the first order Magnus expansion we plotted. This is because the optimal cut-off order of the Magnus expansion (and a number of other high frequency expansions) shrinks with decreasing frequencies [51] unless couplings are small enough to suppress this effect. It should also be noted that the stuttering (wiggles) at low frequencies seen in the plot is an effect that happens because the U_k matrices are relatively small. For larger matrices this averages out as we will see in interacting models to follow. In Fig. 3 we show how well the approximation does as a function of various couplings.

From the plots it is clear that the results obtained via the flow equation approach are generally more accurate than the results from the Magnus expansion. One may worry that for $E \gtrsim 0.4$ sometimes our approximation seems to be outdone by the Magnus approximation. This effect however is of no importance because this is where both approximations are extremely poor and of no use. As expected from general arguments, we find that the approximation does increasingly well for large values of driving h . We now turn to non-integrable models.

B. J_1 - J_2 model with time-dependent magnetic field in x direction

For this model both the Magnus expansion and the flow equation approach yield effective Hamiltonians of the form,

$$H_{\text{eff}} = \sum_{n=1}^2 \sum_i \left(J_n S_i^x S_{i+1}^x + J_n^{y,(a)} S_i^y S_{i+n}^y + J_n^{z,(a)} S_i^z S_{i+n}^z + \Gamma_n^{(a)} (S_i^z S_{i+n}^y + S_i^y S_{i+n}^z) \right), \quad (31)$$

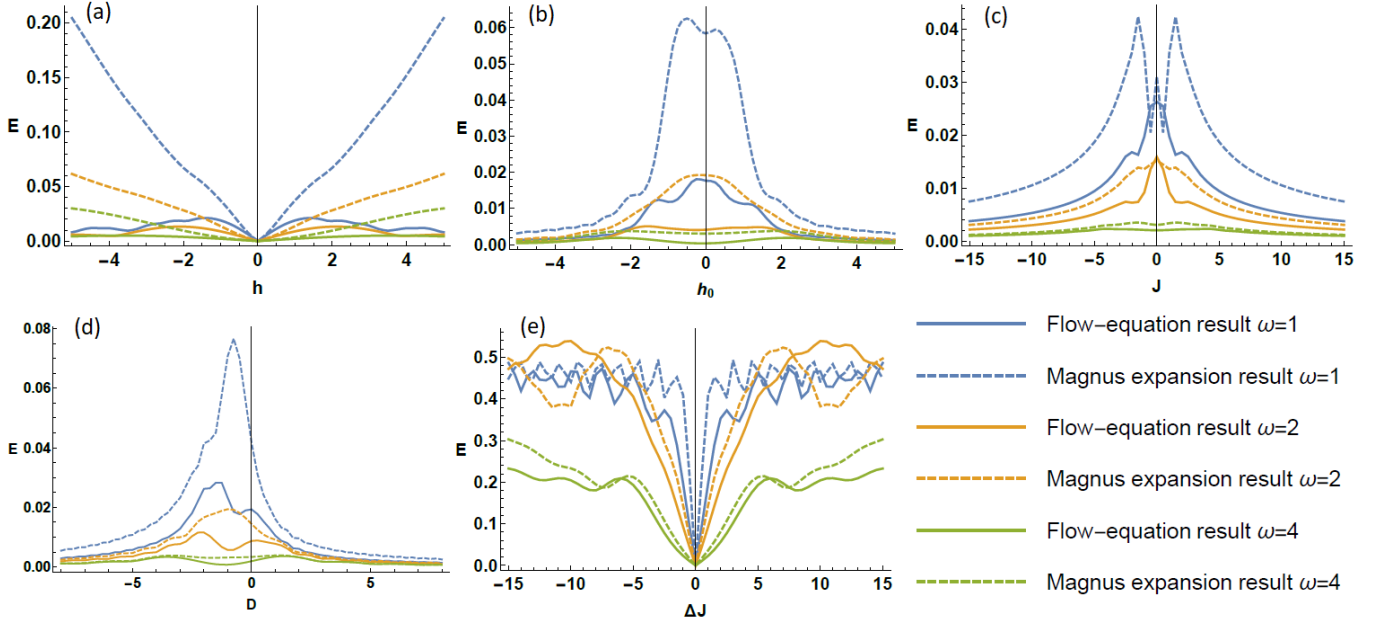


FIG. 3: (Color online.) Relative error E , Eq.(25), as function of the different coupling constants in the Hamiltonian, Eq.(15). Only one coefficient is varied in each subfigure, while the ones that are not varied are fixed at values of $D = 0.1$, $\Delta J = J_x - J_y = 0.1$, $J = \frac{J_x + J_y}{2} = 1.05$, $h_0 = 1$ and $h = 1$. We vary in (a) the driving magnetic field h , (b) the static magnetic field h_0 , (c) the average exchange interaction $J = \frac{J_x + J_y}{2}$, (d) the anti-symmetric exchange strength D and (e) the anisotropy of the exchange interaction $\Delta J = J_x - J_y$.

where (a) labels the approximation scheme (either flow or Magnus). The details of the calculation are again in Appendix A 2.

It is important to note that one of the new terms Γ_n can be removed by a suitable rotation in spin space, which tells us that we went from an XXZ model to a XYZ model followed by a rotation in spin space. The effective coefficients for the Magnus expansion are

$$\begin{aligned} J_n^{y,M} &= J_n, \\ J_n^{z,M} &= J_n^z, \\ \Gamma_n^{(M)} &= B\pi \frac{J_n^z - J_n}{2\omega}, \end{aligned} \quad (32)$$

and for the flow equation approach

$$\begin{aligned} J_n^{y,M} &= \frac{1}{2} \left((J_n^z + J_n) - (J_n^z - J_n) \text{sinc} \left(\frac{2\pi B}{\omega} \right) \right), \\ J_n^{z,M} &= \frac{1}{2} \left((J_n^z + J_n) + (J_n^z - J_n) \text{sinc} \left(\frac{2\pi B}{\omega} \right) \right), \\ \Gamma_n^{(M)} &= \frac{(J_n^z - J_n)\omega \sin^2 \left(\frac{\pi B}{\omega} \right)}{2\pi B}. \end{aligned} \quad (33)$$

Calculating higher orders in the Magnus expansion for this model yields extremely complicated effective Hamiltonians. The second order Magnus expansion already gives a Hamiltonian that is a sum of 60 different operators with complicated prefactors. One tractable way to improve on the first order Magnus expansion is via the

flow equation approach. In Fig. 4 the plots illustrate how well the approximation does for different frequencies. These results are obtained numerically using exact diagonalization for finite size systems, as described in Appendix C.

One finds that the flow equations outperform the Magnus expansion for all frequencies. For the plot of strong driving magnetic field h this is especially pronounced. There the Magnus expansion for a large range of frequencies gives poor results and the flow equations generally give quite precise results.

One may also in this case ask how well the approximation does as a function of all the different coefficients. In Fig. 5, we show a plot for different values of the coefficients. These plots were done only including the sector $k = 0$ in k -space because this is numerically quicker and because other points in k -space reproduce the same results.

Similar to the previous integrable model, for this non-integrable model one can see that the flow equation approach outperforms the Magnus expansion for most parameters. The much higher accuracy for large values of h should be emphasized. The details on how the time evolution operator was obtained are contained in Appendix C.

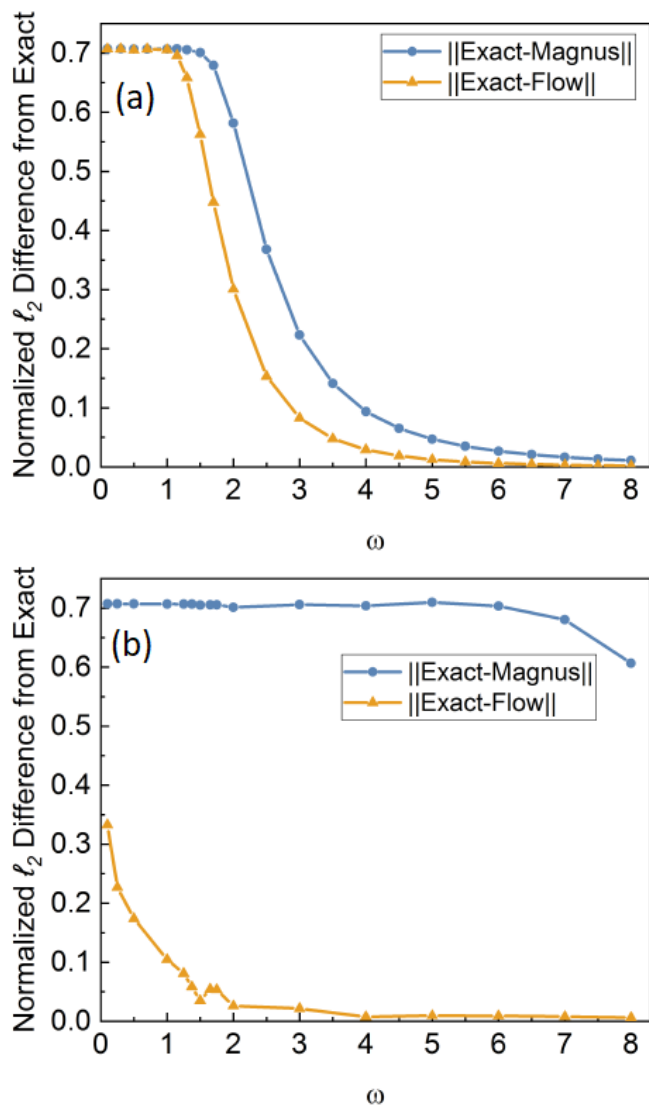


FIG. 4: (Color online.) Plot of the normalized l_2 distance between exact and approximate time evolution operators for a chain of length $L = 16$, and parameters $J_1 = -0.5$, $J_1^z = 1$ and $J_2 = J_2^z = 0$ plotted as a function of frequency for driving magnetic field strengths (a) $B=0.5$ and (b) $B=5$.

C. J_1 - J_2 model with time dependent exchange interaction

Both the Magnus expansion and the flow equations yield an effective Hamiltonian of the form,

$$\begin{aligned}
 H_{eff} = & \sum_i \sum_{n=1}^2 \left\{ J_n^{(a)} \mathbf{S}_i^\perp \mathbf{S}_{i+n}^\perp + J_{z,n}^{(a)} S_i^z S_{i+n}^z \right. \\
 & + D_n^{(a)} [\mathbf{S}_{i+n+1} \times \mathbf{S}_{i+1} + \mathbf{S}_{i-n-1} \times \mathbf{S}_{i-1}]_z S_i^z \\
 & \left. + Q_n^{(a)} [S_i^x S_{i+n}^x + S_i^y S_{i+n}^y] S_{i-1}^z S_{i+n+1}^z \right\}, \quad (34)
 \end{aligned}$$

where $\mathbf{S}_i^\perp = (S_i^x, S_i^y, 0)$ and (a) labels the approximation scheme.

The last two terms of Eq.(34) are newly generated terms in the Hamiltonian. If S_i^z has an approximately uniform orientation the terms proportional to $D_n^{(a)}$ can be interpreted as different range antisymmetric exchange terms - treating S_i^z as a mean field term. By the same token in a mean field approximation the term proportional to $Q_n^{(a)}$ can be interpreted as exchange terms. Beyond the mean-field case it is clear that higher order spin interactions are generated. Such terms can lead to new physics and can drive new phases

The coupling constants within the flow equation approach [solving Eq.(8) exactly] are given by,

$$\begin{aligned}
 J_n^F &= \frac{1}{2} J_n \left[1 + \text{sinc} \left(\frac{\pi J_{1,o}^z}{\omega} \right) \right], \\
 J_{z,1}^F &= J_1^z; \quad J_{z,2}^F = J_2, \\
 D_n^F &= \frac{J_n \omega}{\pi J_{1,o}^z} \left[\cos \left(\frac{\pi J_{1,o}^z}{\omega} \right) - 1 \right], \\
 Q_n^F &= 2J_n \left[1 - \text{sinc} \left(\frac{\pi J_{1,o}^z}{\omega} \right) \right],
 \end{aligned} \quad (35)$$

and within the Magnus expansion,

$$\begin{aligned}
 J_n^M &= J_n; \quad J_{z,1}^F = J_1^z; \quad J_{z,2}^M = J_2, \\
 D_n^M &= -\frac{\pi}{2\omega} J_n J_{1,o}^z; \quad Q_n^M = 0.
 \end{aligned} \quad (36)$$

While the form of the Hamiltonian in Eq.(34) is already complicated it is worth noting that the second order Magnus expansion would become forbiddingly complicated with a sum of over 100 operators, which makes even a numerical implementation impractical. Therefore, the result from the flow equations, while also complicated, is a rather manageable improvement on the first order Magnus expansion.

In Fig.6 we plotted how well the approximation performs for different frequencies.

One finds that the flow equation result is much better in the lower frequency regime and outperforms the Magnus approximation significantly when the external drive is relatively strong. The performance of the two approximations as a function of the different couplings is shown in the plots in Fig.7. Consistent with the models previous discussed, the flow equation approximation does substantially better across all parameter regimes. For this case we made use of the QuSpin package [89] to obtain a comparison to the exact result.

V. COMPARISON WITH RESUMMATIONS OF THE BAKER-CAMPBELL-HAUSDORFF IDENTITY

In this section, we turn the logic around relative to the conventional Hamiltonian-evolution operator relationship. Up to this point in the manuscript, we

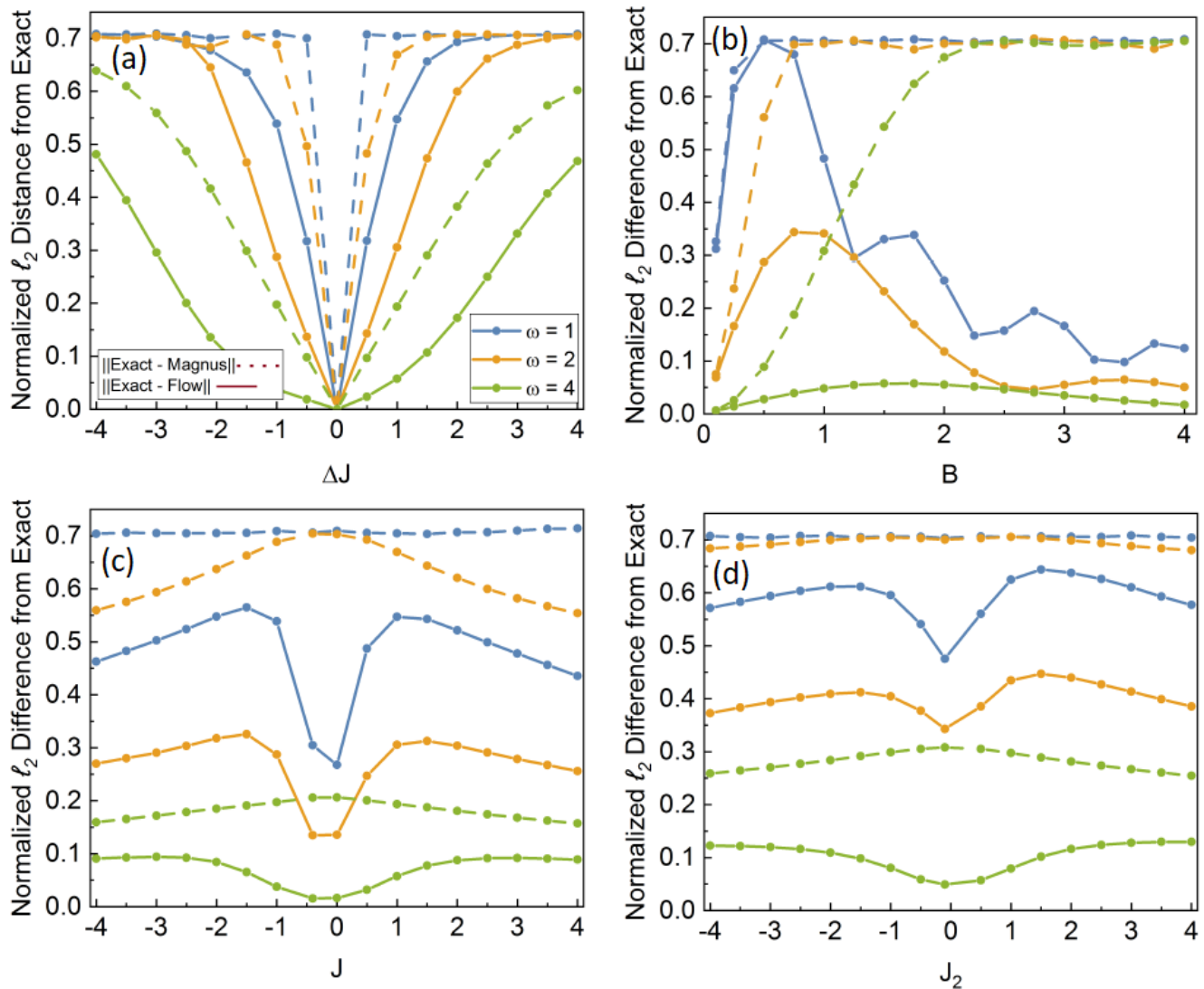


FIG. 5: (Color online.) Plots of the normalized l_2 distance for a chain of length $L = 14$ where we vary the various coupling constants while keeping others fixed. Particularly we are (a) varying nearest neighbor exchange anisotropy $\Delta J = J_1 - J_1^z$, while keeping $B = 1$, average nearest neighbor exchange $J = \frac{J_1 + J_1^z}{2} = 1$ and $J_2 = J_2^z = 0$ fixed, (b) varying B , while keeping $J_1 = -0.5$, $J_1^z = 1$ and $J_2 = J_2^z = 0$ fixed, (c) varying J , while keeping $\Delta J = 1$, $B = 1$ and $J_2 = 0$ fixed and (d) varying J_2 , while keeping $\Delta J = 1$, $B = 1$ and $J = 1$ fixed.

have been asking about computing an effective time-independent Hamiltonian for a time-dependent problem, and we have used this effective Hamiltonian to compute the time evolution of the system. Now, we turn our attention to a situation in which the time evolution operator is known (in our case it takes a specific product form) and we wish to determine an *optimal Hamiltonian* that can be used to produce the desired time evolution.

There has been a recent surge of interest in resummations of the Baker-Campbell-Hausdorff (BCH) identity [88]. An important evolution case where the BCH identity is useful is when the time evolution operator factorizes into a product of matrix exponentials $e^{-iH_1}e^{-iH_2}$. This structure corresponds to multiple dif-

ferent Schrödinger equations. One possible correspondence is to a delta function time dependence in the Schrödinger equation. For example, the kicked transverse field Ising model that is discussed in Ref.[88] has

$$\begin{aligned}
 H_1 &= J \sum_i \sigma_i^z \sigma_{i+1}^z \\
 H_2 &= \sum_i (h_x \sigma_x^i + h_z \sigma_i^z)
 \end{aligned}
 \tag{37}$$

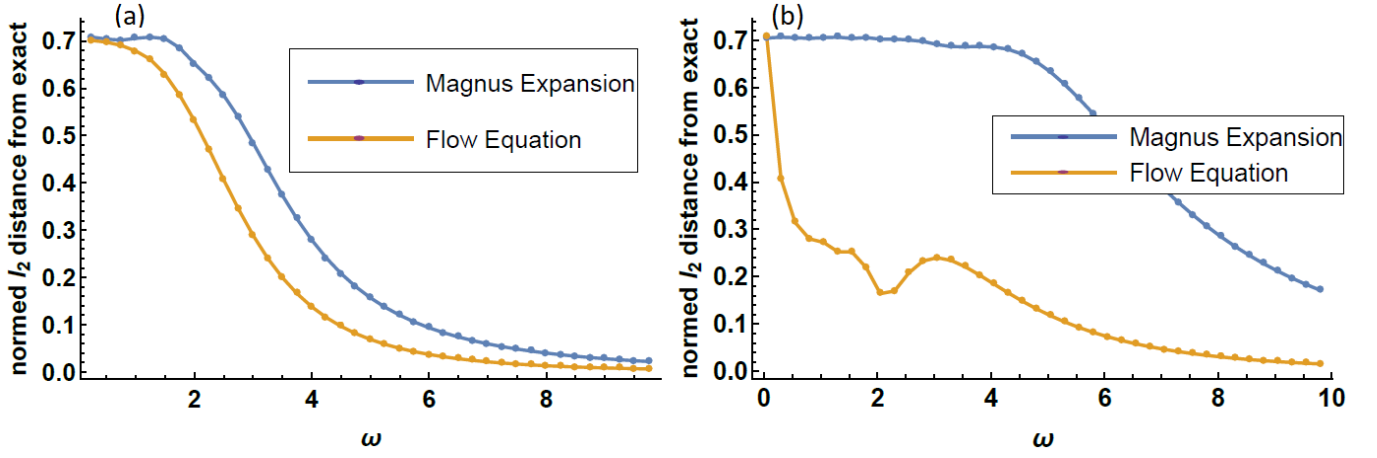


FIG. 6: (Color online.) Plot of the normalized l_2 distance between exact and approximate time evolution operators for $J_1 = 1$, $J_1^z = 2$ and $J_2 = 0.2$ plotted as a function of frequency for a spin chain with $L = 14$ sites. The driving strength of the nearest neighbor exchange term in z-direction is (a) $J_{1,o}^z = 2$ and (b) $J_{1,o}^z = 6$.

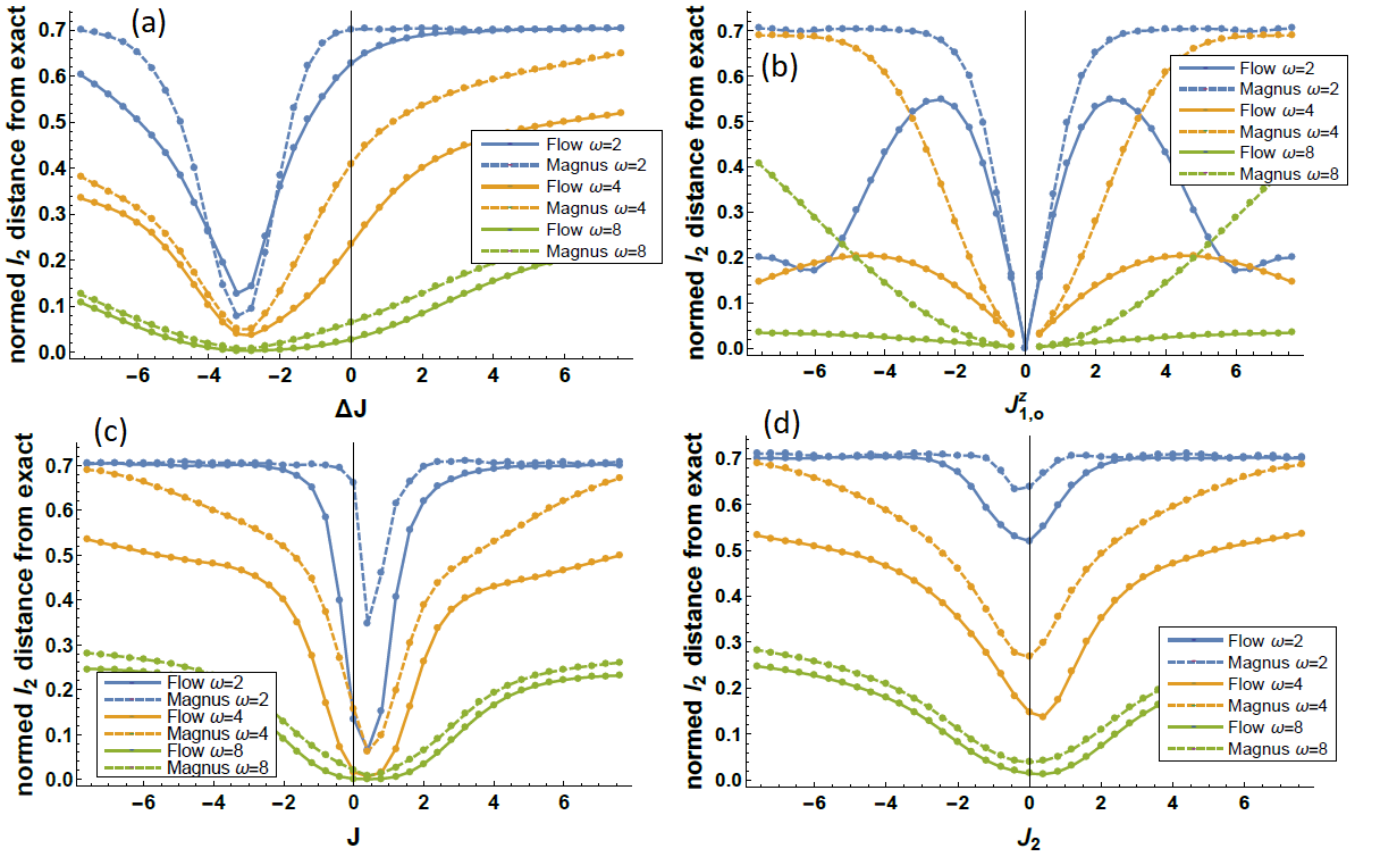


FIG. 7: (Color online.) Shown are plots of the l_2 distance as a function of various coupling constants for a chain of length $L = 14$. In plot (a) we vary the nearest neighbor exchange anisotropy $\Delta J = J_1 - J_1^z$ and keep $J_{1,o}^z = 2$, $J = \frac{1}{2}(J_1 + J_1^z) = 1.5$ and $J_2 = 0.2$ fixed, in (b) we vary the driving strength of the exchange interaction in z-direction $J_{1,o}^z$ and keep $\Delta J = -1$, $J = 1.5$ and $J_2 = 0.2$ fixed, in (c) we vary the average nearest neighbor exchange interaction J and keep $J_{1,o}^z = 2$, $\Delta J = -1$ and $J_2 = 0.2$ fixed and in (d) we vary the next nearest neighbor exchange J_2 while keeping $J_{1,o}^z = 2$, $\Delta J = -1$ and $J = 1.5$ fixed

and can be put into the form,

$$\begin{aligned}
 H(t) &= H_0 + V(t), \\
 H_0 &= \sum_i [J_z \sigma_i^z \sigma_{i+1}^z + h_x \sigma_i^x + h_z \sigma_i^z], \\
 V(t) &= \sum_i [h_x \sigma_i^x + h_z \sigma_i^z] \delta(t-1),
 \end{aligned} \tag{38}$$

where to stay close to the notation of Ref.[88] we use

Pauli operators $\sigma_i^{x,y,z} = 2S_i^{x,y,z}$ rather than the spin operators we used earlier in our manuscript. Here $\delta(t)$ is the Dirac delta function.

Another possibility is to rewrite the problem in terms of a Heaviside θ function as

$$\begin{aligned} H(t) &= H_0 + V(t), \\ H_0 &= \sum_i [J_z \sigma_i^z \sigma_{i+1}^z + h_x \sigma_i^x + h_z \sigma_i^z], \\ V(t) &= \sum_i [h_x \sigma_i^x + h_z \sigma_i^z - J_z \sigma_i^z \sigma_{i+1}^z] (2\theta(t - 1/2) - 1). \end{aligned} \quad (39)$$

Both choices lead to different flow equations and can therefore be interpreted as leading to different resummations of the BCH identity. Thus, we discuss here these two Hamiltonian choices for a given time evolution operator. As a matter of fact, there are infinitely many ways to make a choice in the time dependence, and likely one is an ideal choice. However, we will not discuss this issue of the optimal choice any further.

One finds that within the lowest order in the BCH expansion, the replica approximation used in Ref.[88] and our flow equation approach lead to an approximate Floquet Hamiltonian with the form,

$$\begin{aligned} H_{\text{eff}}^{(a)} &= \sum_i \left[C_x^{(a)} \sigma_i^x + C_z^{(a)} \sigma_i^z + C_{xx}^{(a)} \sigma_i^x \sigma_{i+1}^x \right. \\ &\quad + C_{yy}^{(a)} \sigma_i^y \sigma_{i+1}^y + C_{zz}^{(a)} \sigma_i^z \sigma_{i+1}^z \\ &\quad + C_{xy}^{(a)} \sigma_i^x (\sigma_{i-1}^y + \sigma_{i+1}^y) + C_{xz}^{(a)} \sigma_i^x (\sigma_{i-1}^z + \sigma_{i+1}^z) \\ &\quad \left. + C_{yz}^{(a)} \sigma_i^y (\sigma_{i-1}^z + \sigma_{i+1}^z) + C_{xzz}^{(a)} \sigma_i^x \sigma_{i-1}^z \sigma_{i+1}^z \right], \end{aligned} \quad (40)$$

where a labels the approximation scheme. The different approximations only differ in their coefficients (and some coefficients may be zero). The coefficients themselves offer little to illuminate our discussion. Therefore, their derivation is given in Appendix D.

In Fig. 8 we show a comparative plot for the δ -type and the Heaviside-type resummations. The plots are done for spin chains of length $L = 14$ to get a smooth plot. There are only small numerical differences for longer spin chains.

In the plots one can see that the flow equation approach does better for small values of coupling strength than the Magnus expansion — in some cases also better than the replica expansion. For large couplings, it outperforms both.

From Fig.8, one can see that the flow equation approach is the most reliable approximation with the mismatch in some cases plateauing at values of around 0.1. For those values one is still able to capture at least qualitative features of the time-evolution. Thus, the flow equation approach offers a useful numerical strategy for finding a Hamiltonian describing a given time-evolution. This may be of practical importance in a wide variety of applications where the underlying Hamiltonian may be

hard to determine from microscopic considerations, such as may be the case in various types of quantum information scenarios.

VI. CONCLUSIONS

In conclusion, we have introduced an accurate “flow equation” approach to compute effective time-independent Hamiltonians, valid for finite times (which may be exponentially long) for periodically driven quantum many-particle systems. We have demonstrated the power of the flow equation approach by illustrating how one can reach into perturbatively inaccessible frequency regimes, and shown that the approximation generally yields an improvement over the Magnus expansion. Furthermore, in many instances the results from the flow equation approach also yield a practically accessible improvement on the first order Magnus expansion where no other method appears to be available. A straightforward application of the Magnus expansion leads to an explosion in the number of different operators that contribute to the effective Hamiltonian with coefficients that are tedious to evaluate. In our approach, one is able to truncate the number of operators contributing to the flow equations in a controlled way, which allows one to keep less terms but find highly accurate coefficients. We have also demonstrated that our method compares favorably to resummations of the Baker-Campbell-Hausdorff identity, illustrating it shows its strength even in niche applications, where more powerful methods are to be expected.

In summary, we hope that the demonstration of the validity of our approximate method illustrates its power and potential impact on time-dependent quantum many-body systems. The method is completely general and applicable to any form of time-dependent terms in the Hamiltonian—be it through the potential energy, kinetic energy, or both. With the accurate effective time-independent Hamiltonians that one obtains, new access is granted to potential pre-thermal regimes with properties not present in the equilibrium phase diagram of the original Hamiltonian. Our results also open the door to new opportunities for quantum control through Hamiltonian engineering to create desired properties out-of-equilibrium. The effective Hamiltonian can be used to compute any observable over finite times through the standard formulas of statistical mechanics, in addition to accurately governing the evolution of the quantum states themselves. We hope our approach will inspire new studies that exploit its flexibility and may even expand the range of approximation schemes that can be employed within it. With it, new regimes of cold atom, condensed matter, and other systems will likely be uncovered and exploited.

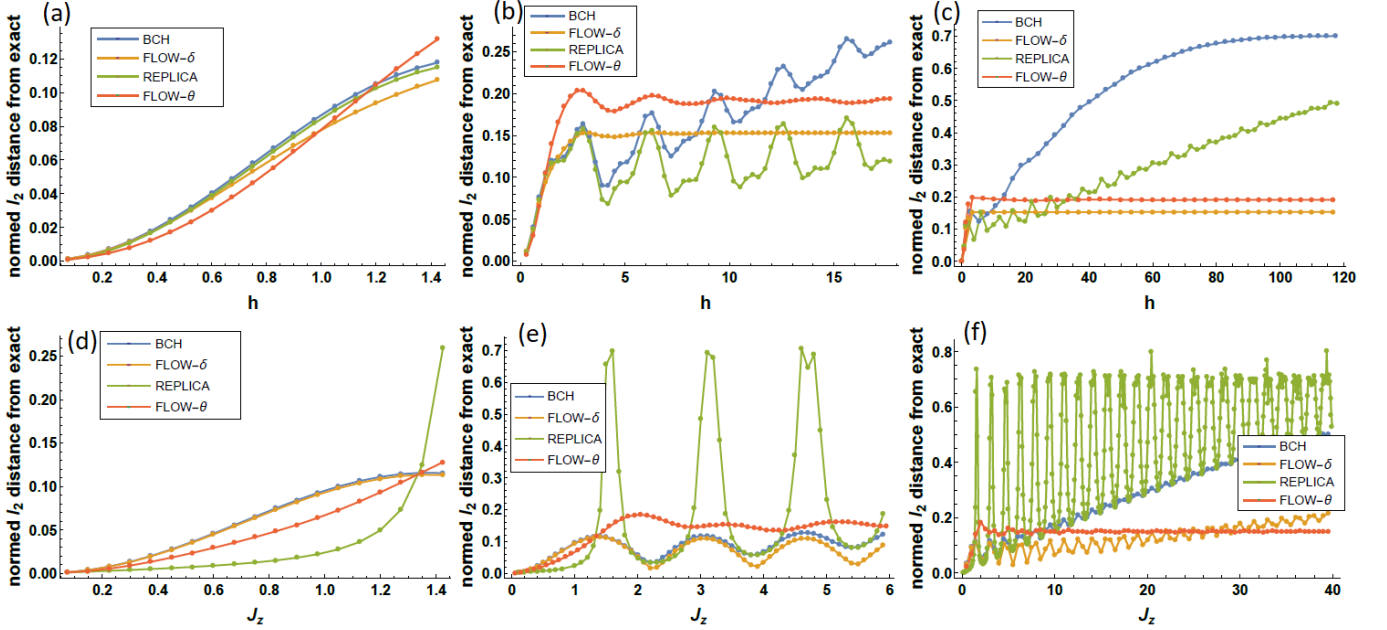


FIG. 8: (Color online.) Plot of the normalized l_2 distance between the exact time evolution operator and the approximate time evolution operator for $h_x = h \cos \theta$, $h_z = h \sin \theta$, and $\theta = 0.643501$ using the “ δ -formulation” of the flow equations in orange and the “Heaviside θ -formulation” in red. In plots (a-c) we keep $J_z = 0.1$ fixed and plot different ranges of h values, which are (a) short range h , (b) medium range h and (c) long range h . Similarly in plots (d-f) we keep $h = 0.1$ fixed and plot different ranges of J_z values, which are (d) short range J_z , (e) medium range J_z and (f) long range J_z .

Acknowledgments

We gratefully acknowledge funding from Army Research Office Grant No. W911NF-14-1-0579, NSF Grant No. DMR-1507621, and NSF Materials Research Science and Engineering Center Grant No. DMR-1720595.

We acknowledge the Texas Advanced Computing Center (TACC) at The University of Texas at Austin for providing computing resources that have contributed to the research results reported within this paper. www.tacc.utexas.edu GAF acknowledges support from a Simons Fellowship.

-
- [1] A. Polkovnikov, K. Sengupta, A. Silva, and M. Vengalattore, *Rev. Mod. Phys.* **83**, 863 (2011), URL <http://link.aps.org/doi/10.1103/RevModPhys.83.863>.
- [2] A. Eckardt, *Rev. Mod. Phys.* **89**, 011004 (2017), URL <https://link.aps.org/doi/10.1103/RevModPhys.89.011004>.
- [3] I. Bloch, J. Dalibard, and W. Zwerger, *Rev. Mod. Phys.* **80**, 885 (2008), URL <http://link.aps.org/doi/10.1103/RevModPhys.80.885>.
- [4] J. Dalibard, F. Gerbier, G. Juzeliūnas, and P. Öhberg, *Rev. Mod. Phys.* **83**, 1523 (2011), URL <http://link.aps.org/doi/10.1103/RevModPhys.83.1523>.
- [5] D. N. Basov, R. D. Averitt, and D. Hsieh, *Nat. Mat.* **16**, 1077 (2017).
- [6] J. Zhang and R. Averitt, *Annu. Rev. Mater. Res.* **44**, 19 (2014), URL <https://doi.org/10.1146/annurev-matsci-070813-113258>.
- [7] D. N. Basov, R. D. Averitt, D. van der Marel, M. Dressel, and K. Haule, *Rev. Mod. Phys.* **83**, 471 (2011), URL <https://link.aps.org/doi/10.1103/RevModPhys.83.471>.
- [8] C. Giannetti, M. Capone, D. Fausti, M. Fabrizio, F. Parmigiani, and D. Mihailovic, *Adv. Phys.* **65**, 58 (2016), URL <http://dx.doi.org/10.1080/00018732.2016.1194044>.
- [9] M. Gandolfi, G. L. Celardo, F. Borgonovi, G. Ferrini, A. Avella, F. Banfi, and C. Giannetti, *Phys. Scr.* **92**, 034004 (2017), URL <http://stacks.iop.org/1402-4896/92/i=3/a=034004>.
- [10] J. H. Mentink and M. Eckstein, *Phys. Rev. Lett.* **113**, 057201 (2014), URL <http://link.aps.org/doi/10.1103/PhysRevLett.113.057201>.
- [11] J. Mentink, K. Balzer, and M. Eckstein, *Nat. Comms.* **6**, 6708 (2015).
- [12] D. Fausti, R. I. Tobey, N. Dean, S. Kaiser, A. Dienst, M. C. Hoffmann, S. Pyon, T. Takayama, H. Takagi, and A. Cavalleri, *Science* **331**, 189 (2011), ISSN 0036-8075, URL <http://science.sciencemag.org/content/331/6014/189>.
- [13] A. Cavalleri, *Contemp. Phys.* **59**, 31 (2018), URL <https://doi.org/10.1080/00344894.2018.1511111>.

- //doi.org/10.1080/00107514.2017.1406623.
- [14] L. Stojchevska, I. Vaskivskiy, T. Mertelj, P. Kusar, D. Svetin, S. Brazovskii, and D. Mihailovic, *Science* **344**, 177 (2014), ISSN 0036-8075, URL <http://science.sciencemag.org/content/344/6180/177>.
- [15] Y. A. Gerasimenko, I. Vaskivskiy, and D. Mihailovic (2017), arXiv:1704.08149, URL <https://arxiv.org/abs/1704.08149>.
- [16] J. Zhang, P. W. Hess, A. Kyprianidis, P. Becker, A. Lee, J. Smith, G. Pagano, I.-D. Potirniche, A. C. Potter, A. Vishwanath, et al., *Nature* **543**, 217 (2017).
- [17] S. Choi, J. Choi, R. Landig, G. Kucsko, H. Zhou, J. Isoya, F. Jelezko, S. Onoda, H. Sumiya, V. Khemani, et al., *Nature* **543**, 221 (2017).
- [18] A. C. Potter, T. Morimoto, and A. Vishwanath, *Phys. Rev. X* **6**, 041001 (2016), URL <http://link.aps.org/doi/10.1103/PhysRevX.6.041001>.
- [19] V. Khemani, A. Lazarides, R. Moessner, and S. L. Sondhi, *Phys. Rev. Lett.* **116**, 250401 (2016), URL <http://link.aps.org/doi/10.1103/PhysRevLett.116.250401>.
- [20] M. Bukov, L. D'Alessio, and A. Polkovnikov, *Adv. Phys.* **64**, 139 (2015), URL <http://dx.doi.org/10.1080/00018732.2015.1055918>.
- [21] J. H. Shirley, *Phys. Rev.* **138**, B979 (1965), URL <http://link.aps.org/doi/10.1103/PhysRev.138.B979>.
- [22] R. Moessner and S. L. Sondhi, *Nat. Phys.* **13**, 424 (2017).
- [23] A. Lazarides, A. Das, and R. Moessner, *Phys. Rev. Lett.* **112**, 150401 (2014), URL <http://link.aps.org/doi/10.1103/PhysRevLett.112.150401>.
- [24] W. Berdanier, M. Kolodrubetz, R. Vasseur, and J. E. Moore, *Phys. Rev. Lett.* **118**, 260602 (2017), URL <https://link.aps.org/doi/10.1103/PhysRevLett.118.260602>.
- [25] P. Ponte, A. Chandran, Z. Papi, and D. A. Abanin, *Ann. Phys. (N.Y.)* **353**, 196 (2015), ISSN 0003-4916, URL <http://www.sciencedirect.com/science/article/pii/S0003491614003212>.
- [26] P. Ponte, Z. Papić, F. m. c. Huvneers, and D. A. Abanin, *Phys. Rev. Lett.* **114**, 140401 (2015), URL <http://link.aps.org/doi/10.1103/PhysRevLett.114.140401>.
- [27] A. Lazarides, A. Das, and R. Moessner, *Phys. Rev. E* **90**, 012110 (2014), URL <http://link.aps.org/doi/10.1103/PhysRevE.90.012110>.
- [28] Y. H. Wang, H. Steinberg, P. Jarillo-Herrero, and N. Gedik, *Science* **342**, 453 (2013), ISSN 0036-8075, URL <http://science.sciencemag.org/content/342/6157/453>.
- [29] L. Jiang, T. Kitagawa, J. Alicea, A. R. Akhmerov, D. Pekker, G. Refael, J. I. Cirac, E. Demler, M. D. Lukin, and P. Zoller, *Phys. Rev. Lett.* **106**, 220402 (2011), URL <https://link.aps.org/doi/10.1103/PhysRevLett.106.220402>.
- [30] P. Mognini, E. van Nieuwenburg, and R. Chitra, *Phys. Rev. B* **96**, 125144 (2017), URL <https://link.aps.org/doi/10.1103/PhysRevB.96.125144>.
- [31] K. Jiménez-García, L. J. LeBlanc, R. A. Williams, M. C. Beeler, C. Qu, M. Gong, C. Zhang, and I. B. Spielman, *Phys. Rev. Lett.* **114**, 125301 (2015), URL <http://link.aps.org/doi/10.1103/PhysRevLett.114.125301>.
- [32] J. Klinovaja, P. Stano, and D. Loss, *Phys. Rev. Lett.* **116**, 176401 (2016), URL <http://link.aps.org/doi/10.1103/PhysRevLett.116.176401>.
- [33] L. Du, X. Zhou, and G. A. Fiete, *Phys. Rev. B* **95**, 035136 (2017), URL <http://link.aps.org/doi/10.1103/PhysRevB.95.035136>.
- [34] Q. Chen, L. Du, and G. A. Fiete, *Phys. Rev. B* **97**, 035422 (2018), URL <https://link.aps.org/doi/10.1103/PhysRevB.97.035422>.
- [35] P. Titum, E. Berg, M. S. Rudner, G. Refael, and N. H. Lindner, *Phys. Rev. X* **6**, 021013 (2016), URL <https://link.aps.org/doi/10.1103/PhysRevX.6.021013>.
- [36] L. D'Alessio and M. Rigol, *Nat. Comms.* **6**, 8836 (2015).
- [37] I. Martin, G. Refael, and B. Halperin, *Phys. Rev. X* **7**, 041008 (2017), URL <https://link.aps.org/doi/10.1103/PhysRevX.7.041008>.
- [38] T. Oka and H. Aoki, *Phys. Rev. B* **79**, 081406 (2009), URL <http://link.aps.org/doi/10.1103/PhysRevB.79.081406>.
- [39] N. H. Lindner, G. Refael, and V. Galitski, *Nat. Phys.* **7**, 490 (2011).
- [40] T. Kitagawa, T. Oka, A. Brataas, L. Fu, and E. Demler, *Phys. Rev. B* **84**, 235108 (2011), URL <http://link.aps.org/doi/10.1103/PhysRevB.84.235108>.
- [41] Z. Gu, H. A. Fertig, D. P. Arovas, and A. Auerbach, *Phys. Rev. Lett.* **107**, 216601 (2011), URL <https://link.aps.org/doi/10.1103/PhysRevLett.107.216601>.
- [42] M. S. Rudner, N. H. Lindner, E. Berg, and M. Levin, *Phys. Rev. X* **3**, 031005 (2013), URL <https://link.aps.org/doi/10.1103/PhysRevX.3.031005>.
- [43] G. Usaj, P. M. Perez-Piskunow, L. E. F. Foa Torres, and C. A. Balseiro, *Phys. Rev. B* **90**, 115423 (2014), URL <http://link.aps.org/doi/10.1103/PhysRevB.90.115423>.
- [44] A. Zenesini, H. Lignier, D. Ciampini, O. Morsch, and E. Arimondo, *Phys. Rev. Lett.* **102**, 100403 (2009), URL <https://link.aps.org/doi/10.1103/PhysRevLett.102.100403>.
- [45] A. Eckardt, C. Weiss, and M. Holthaus, *Phys. Rev. Lett.* **95**, 260404 (2005), URL <https://link.aps.org/doi/10.1103/PhysRevLett.95.260404>.
- [46] N. Y. Yao, A. C. Potter, I.-D. Potirniche, and A. Vishwanath, *Phys. Rev. Lett.* **118**, 030401 (2017), URL <https://link.aps.org/doi/10.1103/PhysRevLett.118.030401>.
- [47] I.-D. Potirniche, A. C. Potter, M. Schleier-Smith, A. Vishwanath, and N. Y. Yao, *Phys. Rev. Lett.* **119**, 123601 (2017), URL <https://link.aps.org/doi/10.1103/PhysRevLett.119.123601>.
- [48] J. Rehn, A. Lazarides, F. Pollmann, and R. Moessner, *Phys. Rev. B* **94**, 020201 (2016), URL <http://link.aps.org/doi/10.1103/PhysRevB.94.020201>.
- [49] L. D'Alessio and M. Rigol, *Phys. Rev. X* **4**, 041048 (2014), URL <http://link.aps.org/doi/10.1103/PhysRevX.4.041048>.
- [50] D. A. Abanin, W. De Roeck, and F. m. c. Huvneers, *Phys. Rev. Lett.* **115**, 256803 (2015), URL <http://link.aps.org/doi/10.1103/PhysRevLett.115.256803>.
- [51] D. A. Abanin, W. De Roeck, W. W. Ho, and F. m. c. Huvneers, *Phys. Rev. B* **95**, 014112 (2017), URL <https://link.aps.org/doi/10.1103/PhysRevB.95.014112>.
- [52] T. Mori, T. Kuwahara, and K. Saito, *Phys. Rev. Lett.* **116**, 120401 (2016), URL <https://link.aps.org/doi/10.1103/PhysRevLett.116.120401>.
- [53] D. V. Else, B. Bauer, and C. Nayak, *Phys. Rev. X* **7**, 011026 (2017), URL <https://link.aps.org/doi/10.1103/PhysRevX.7.011026>.
- [54] E. Canovi, M. Kollar, and M. Eckstein, *Phys. Rev. E*

- 93, 012130 (2016), URL <https://link.aps.org/doi/10.1103/PhysRevE.93.012130>.
- [55] F. Machado, G. D. Meyer, D. V. Else, C. Nayak, and N. Y. Yao (2017), arXiv:1708.01620, URL <https://arxiv.org/abs/1708.01620>.
- [56] S. A. Weidinger and M. Knap, Sci. Rep. **7**, 45382 (2017).
- [57] T. Kuwahara, T. Mori, and K. Saito, Ann. Phys. (N.Y.) **367**, 96 (2016), ISSN 0003-4916, URL <http://www.sciencedirect.com/science/article/pii/S0003491616000142>.
- [58] M. Heyl, A. Polkovnikov, and S. Kehrein, Phys. Rev. Lett. **110**, 135704 (2013), URL <http://link.aps.org/doi/10.1103/PhysRevLett.110.135704>.
- [59] P. Jurcevic, H. Shen, P. Hauke, C. Maier, T. Brydges, C. Hempel, B. P. Lanyon, M. Heyl, R. Blatt, and C. F. Roos, Phys. Rev. Lett. **119**, 080501 (2017), URL <https://link.aps.org/doi/10.1103/PhysRevLett.119.080501>.
- [60] N. Fläschner, D. Vogel, M. Tarnowski, B. S. Rem, D.-S. Lühmann, M. Heyl, J. C. Budich, L. Mathey, K. Senegstock, and C. Weitenberg, Nat. Phys. **14**, 265 (2018), URL <https://arxiv.org/abs/1608.05616>.
- [61] L. Du and G. A. Fiete, Phys. Rev. B **97**, 085152 (2018), URL <https://link.aps.org/doi/10.1103/PhysRevB.97.085152>.
- [62] Y.-A. Chen, S. Nascimbène, M. Aidelsburger, M. Atala, S. Trotzky, and I. Bloch, Phys. Rev. Lett. **107**, 210405 (2011), URL <https://link.aps.org/doi/10.1103/PhysRevLett.107.210405>.
- [63] C. Dutreix and M. I. Katsnelson, Phys. Rev. B **95**, 024306 (2017), URL <http://link.aps.org/doi/10.1103/PhysRevB.95.024306>.
- [64] M. Bukov, S. Gopalakrishnan, M. Knap, and E. Demler, Phys. Rev. Lett. **115**, 205301 (2015), URL <https://link.aps.org/doi/10.1103/PhysRevLett.115.205301>.
- [65] M. Bukov, M. Kolodrubetz, and A. Polkovnikov, Phys. Rev. Lett. **116**, 125301 (2016), URL <https://link.aps.org/doi/10.1103/PhysRevLett.116.125301>.
- [66] F. Peronaci, M. Schiró, and O. Parcollet (2017), arXiv:1711.07889, URL <https://arxiv.org/abs/1711.07889>.
- [67] N. H. Lindner, E. Berg, and M. S. Rudner, Phys. Rev. X **7**, 011018 (2017), URL <https://link.aps.org/doi/10.1103/PhysRevX.7.011018>.
- [68] K. Plekhanov, G. Roux, and K. Le Hur, Phys. Rev. B **95**, 045102 (2017), URL <https://link.aps.org/doi/10.1103/PhysRevB.95.045102>.
- [69] S. Blanes, F. Casas, J. Oteo, and J. Ros, Phys. Rep. **470**, 151 (2009), ISSN 0370-1573, URL <http://www.sciencedirect.com/science/article/pii/S0370157308004092>.
- [70] E. Fel'dman, Phys. Lett. A **104**, 479 (1984), ISSN 0375-9601, URL <http://www.sciencedirect.com/science/article/pii/0375960184900276>.
- [71] W. Magnus, Commun. Pure Appl. Math. **7**, 649 (1954), ISSN 1097-0312, URL <http://dx.doi.org/10.1002/cpa.3160070404>.
- [72] S. Rahav, I. Gilary, and S. Fishman, Phys. Rev. A **68**, 013820 (2003), URL <http://link.aps.org/doi/10.1103/PhysRevA.68.013820>.
- [73] N. Goldman and J. Dalibard, Phys. Rev. X **4**, 031027 (2014), URL <http://link.aps.org/doi/10.1103/PhysRevX.4.031027>.
- [74] A. P. Itin and M. I. Katsnelson, Phys. Rev. Lett. **115**, 075301 (2015), URL <http://link.aps.org/doi/10.1103/PhysRevLett.115.075301>.
- [75] A. Eckardt and E. Anisimovas, New J. of Phys. **17**, 093039 (2015), URL <http://stacks.iop.org/1367-2630/17/i=9/a=093039>.
- [76] T. Mikami, S. Kitamura, K. Yasuda, N. Tsuji, T. Oka, and H. Aoki, Phys. Rev. B **93**, 144307 (2016), URL <http://link.aps.org/doi/10.1103/PhysRevB.93.144307>.
- [77] P. Mohan, R. Saxena, A. Kundu, and S. Rao, Phys. Rev. B **94**, 235419 (2016), URL <http://link.aps.org/doi/10.1103/PhysRevB.94.235419>.
- [78] M. M. Maricq, Phys. Rev. B **25**, 6622 (1982), URL <http://link.aps.org/doi/10.1103/PhysRevB.25.6622>.
- [79] P. Bordia, H. Lüschen, U. Schneider, M. Knap, and I. Bloch, Nat. Phys. **13**, 460 (2017).
- [80] N. Goldman, J. Dalibard, M. Aidelsburger, and N. R. Cooper, Phys. Rev. A **91**, 033632 (2015), URL <https://link.aps.org/doi/10.1103/PhysRevA.91.033632>.
- [81] R. Shankar, Rev. Mod. Phys. **66**, 129 (1994), URL <http://link.aps.org/doi/10.1103/RevModPhys.66.129>.
- [82] F. Wegner, Ann. der Phys. (Leipzig) **3**, 77 (1994).
- [83] S. Kehrein, *The Flow Equation Approach to Many-Particle Systems*, Springer Tracts in Modern Physics (Springer Berlin Heidelberg, 2007), ISBN 9783540340683, URL <https://books.google.com/books?id=haH1BwAAQBAJ>.
- [84] S. J. Thomson and M. Schiró, Phys. Rev. B **97**, 060201 (2018), URL <https://link.aps.org/doi/10.1103/PhysRevB.97.060201>.
- [85] T. Giamarchi, *Quantum Physics in One Dimension*, International series of monographs on physics (Oxford University Press, 2004), ISBN 9780198525004, URL <http://books.google.com/books?id=GVeukZLGMZOC>.
- [86] K. Nomura and K. Okamoto, J. Phys. Soc. Jap. **62**, 1123 (1993), URL <https://doi.org/10.1143/JPSJ.62.1123>.
- [87] F. D. M. Haldane, Phys. Rev. B **25**, 4925 (1982), URL <https://link.aps.org/doi/10.1103/PhysRevB.25.4925>.
- [88] S. Vajna, K. Klobas, T. c. v. Prosen, and A. Polkovnikov, Phys. Rev. Lett. **120**, 200607 (2018), URL <https://link.aps.org/doi/10.1103/PhysRevLett.120.200607>.
- [89] P. Weinberg and M. Bukov, SciPost Phys. **2**, 003 (2017), URL <https://scipost.org/10.21468/SciPostPhys.2.1.003>.
- [90] A. W. Sandvik, AIP Conference Proceedings **1297**, 135 (2010).
- [91] C. Zhang, F. Pollmann, S. L. Sondhi, and R. Moessner, Ann. Phys. (Leipzig) **529**, 1600294 (2017).
- [92] H. De Raedt and B. De Raedt, Phys. Rev. A **28**, 3575 (1983), URL <http://link.aps.org/doi/10.1103/PhysRevA.28.3575>.
- [93] E. Polizzi, Phys. Rev. B **79**, 115112 (2009), URL <http://link.aps.org/doi/10.1103/PhysRevB.79.115112>.

Appendix A: Effective Hamiltonians

For the lowest order Magnus expansion the effective Hamiltonian is,

$$H_{\text{eff}} = \frac{1}{T} \int_0^t dt \left(H(t) + i \int_0^t dt_1 [H(t_1), H(t)] \right). \quad (\text{A1})$$

This will be a reference point for our flow equation approach.

1. Flow equation approach for the XY-spin chain with anti-symmetric exchange

We find that at each flow-step of Eq.(8) the Hamiltonian $H(s)$ retains the form

$$H(s, t) = \sum_i (c_1(s, t) S_i^x S_{i+1}^x + c_2(s, t) S_i^y S_{i+1}^y + c_3(s, t) S_i^x S_{i+1}^y + c_4(s, t) S_i^y S_{i+1}^x + c_5(s, t) S_i^z), \quad (\text{A2})$$

where our initial Hamiltonian, Eq.(15), tells us that we have the initial conditions

$$\begin{aligned} c_1(0, t) &= J_x, \\ c_2(0, t) &= J_y, \\ c_3(0, t) &= D, \\ c_4(0, t) &= -D, \\ c_5(0, t) &= h_0 + h(t). \end{aligned} \quad (\text{A3})$$

Defining $h_I(t) := \int_0^t dt' h(t')$ we can compactly write the flow equations for the coefficients as

$$\begin{aligned} \frac{dc_1(s, t)}{ds} &= h_I(t) \cdot (c_3(s, t) + c_4(s, t)), \\ \frac{dc_2(s, t)}{ds} &= -h_I(t) \cdot (c_3(s, t) + c_4(s, t)), \\ \frac{dc_3(s, t)}{ds} &= h_I(t) \cdot (c_2(s, t) - c_1(s, t)), \\ \frac{dc_4(s, t)}{ds} &= h_I(t) \cdot (c_2(s, t) - c_1(s, t)), \\ \frac{dc_5(s, t)}{ds} &= -h(t). \end{aligned} \quad (\text{A4})$$

The solution at $s = 1$ is found as

$$\begin{aligned} c_1(1, t) &= J + \frac{\Delta J}{2} \cos(2h_I(t)), \\ c_2(1, t) &= J - \frac{\Delta J}{2} \cos(2h_I(t)), \\ c_3(1, t) &= D - \frac{\Delta J}{2} \sin(2h_I(t)), \\ c_4(1, t) &= -D - \frac{\Delta J}{2} \sin(2h_I(t)), \\ c_5(1, t) &= h_0. \end{aligned} \quad (\text{A5})$$

Taking the explicit form $h(t) = h \sin(\omega t)$, we can take a time average over a period of the Hamiltonian and find

the approximate Hamiltonian at stroboscopic times as

$$\begin{aligned} H_{\text{eff}} &= \sum_i (J_x^{(f)} S_i^x S_{i+1}^x + J_y^{(f)} S_i^y S_{i+1}^y + D_+^{(f)} S_i^x S_{i+1}^y \\ &\quad + D_-^{(f)} S_i^y S_{i+1}^x + h_0 S_i^z), \\ J_x^{(f)} &:= J + \frac{\Delta J}{2} \cos\left(\frac{2h}{\omega}\right) J_0\left(\frac{2h}{\omega}\right), \\ J_y^{(f)} &:= J - \frac{\Delta J}{2} \cos\left(\frac{2h}{\omega}\right) J_0\left(\frac{2h}{\omega}\right), \\ D_{\pm}^{(f)} &:= \pm D - \frac{\Delta J}{2} \sin\left(\frac{2h}{\omega}\right) J_0\left(\frac{2h}{\omega}\right). \end{aligned} \quad (\text{A6})$$

2. Flow equation approach for the $J_1 - J_2$ model with time dependent magnetic field in x -direction

We find that at each flow-step [using Eq.(8)] the Hamiltonian has the form,

$$\begin{aligned} H(s, t) &= \sum_n \sum_i (C_{xx}^n(s, t) S_i^x S_{i+n}^x + C_{yy}^n(s, t) S_i^y S_{i+n}^y \\ &\quad + C_{zz}^n(s, t) S_i^z S_{i+n}^z + C_{yz}^n(s, t) (S_i^z S_{i+n}^y + S_i^y S_{i+n}^z)) \\ &\quad + \sum_i \tilde{h}(s, t) S_i^z, \end{aligned} \quad (\text{A7})$$

where our initial Hamiltonian, Eq.(18), gives us the boundary conditions

$$\begin{aligned} C_{xx}^n(0, t) &= J_n, \\ C_{yy}^n(0, t) &= J_n, \\ C_{zz}^n(0, t) &= \Delta J_n, \\ C_{yz}^n(0, t) &= 0, \\ \tilde{h}(0, t) &= h(t). \end{aligned} \quad (\text{A8})$$

Defining $h_I(t) := \int_0^t dt' h(t')$ we find that an infinitesimal step implies the flow equations

$$\begin{aligned} \frac{dC_{xx}^n(s, t)}{ds} &= 0, \\ \frac{dC_{yy}^n(s, t)}{ds} &= 2h_I(t) \cdot C_{yz}^n(s, t), \\ \frac{dC_{zz}^n(s, t)}{ds} &= -2h_I(t) \cdot C_{yz}^n(s, t), \\ \frac{dC_{yz}^n(s, t)}{ds} &= -h_I(t) \cdot (C_{yy}^n(s, t) - C_{zz}^n(s, t)), \\ \frac{d\tilde{h}(s, t)}{ds} &= -h(t). \end{aligned} \quad (\text{A9})$$

The solution at $s = 1$ is found as

$$\begin{aligned}
C_{xx}^n(1, t) &= J_n, \\
C_{yy}^n(1, t) &= \frac{J_n}{2} (2 + 2J_n^z - 1) \sin^2(h_I(t)), \\
C_{zz}^n(1, t) &= \frac{J_n}{2} (2 + 2(J_n^z - 1) \cos^2(h_I(t))), \\
C_{yz}^n(1, t) &= \frac{J_n}{2} (J_n^z - 1) \sin(2h_I(t)), \\
\tilde{h}(1, t) &= 0
\end{aligned} \tag{A10}$$

For the special case of

$$h(t) = B \begin{cases} 1; & 2n\pi < \omega t < 2n\pi + \pi \\ -1; & 2n\pi + \pi < \omega t < 2(n+1)\pi \end{cases} ; \quad n \in \mathbb{Z} \tag{A11}$$

we find

$$\begin{aligned}
H_{\text{eff}} &= \sum_{n=1}^2 \sum_i (J_n S_i^x S_{i+1}^x + J_n^y S_i^y S_{i+n}^y + J_n^z S_i^z S_{i+n}^z \\
&\quad + \Gamma_n (S_i^z S_{i+n}^y + S_i^y S_{i+n}^z)), \\
J_n^y &:= \frac{J_n}{4} \left(2J_n^z - \frac{(J_n^z - 1)\omega \sin\left(\frac{2\pi B}{\omega}\right)}{\pi B} + 2 \right), \\
J_n^z &:= \frac{J_n \left((J_n^z - 1)\omega \sin\left(\frac{2\pi B}{\omega}\right) + 2\pi(J_n^z + 1)B \right)}{4\pi B}, \\
\Gamma_n &:= \frac{(J_n^z - 1)J_n \omega \sin^2\left(\frac{\pi B}{\omega}\right)}{2\pi B}.
\end{aligned} \tag{A12}$$

Appendix B: Time evolution operator for the XY model with time-dependent magnetic field in z-direction

The equation for the time evolution operator in this case has the form

$$i\partial_t U(t) = \sum_k H_k U(t), \tag{B1}$$

with $[H_k, H_{k'}] = 0, \forall k \neq k'$. One may make a separation of variables ansatz

$$U = \prod_k U_k, \tag{B2}$$

where we assume that $[U_k, U_{k'}] = 0, \forall k \neq k'$. Inserting this ansatz into Eq.(B1) gives

$$i \sum_k (\partial_t U_k) \left[\prod_{k' \neq k} U_{k'} \right] = \sum_k H_k U_k \left[\prod_{k' \neq k} U_{k'} \right]. \tag{B3}$$

It is a sufficient condition for this equation to be fulfilled that it is satisfied term by term. This yields

$$i(\partial_t U_k) = H_k(t) U_k. \tag{B4}$$

In our case generically $H_k(t)$ has the form

$$H_k(t) = (c_k^\dagger, c_{-k}) \begin{pmatrix} H_{11}^k(t) & H_{12}^k(t) \\ H_{21}^k(t) & H_{22}^k(t) \end{pmatrix} \begin{pmatrix} c_k \\ c_{-k}^\dagger \end{pmatrix}. \tag{B5}$$

An ansatz for U_k therefore is

$$\begin{aligned}
U_k(t) &= A_0^k(t) + A_1^k(t) c_k^\dagger c_k + A_2^k(t) c_{-k}^\dagger c_{-k} + A_3^k(t) c_{-k} c_k \\
&\quad + A_4^k(t) c_{-k}^\dagger c_k^\dagger + A_5^k(t) c_{-k}^\dagger c_k^\dagger c_{-k} c_k,
\end{aligned} \tag{B6}$$

which indeed fulfills $[U_k, U_{k'}] = 0, \forall k \neq k'$. Inserting the ansatz in Eq.(B4) we find that it is consistent since no further terms appear. By equating coefficients we find

$$\frac{\partial \mathbf{A}^k(t)}{\partial t} = i \begin{pmatrix} -H_{22}^k(t) & 0 & 0 & 0 & H_{21}^k(t) & 0 \\ -H_{11}^k(t) & -H_{11}^k(t) - H_{22}^k(t) & 0 & 0 & -H_{21}^k(t) & 0 \\ H_{22}^k(t) & 0 & 0 & 0 & -H_{21}^k(t) & 0 \\ -H_{21}^k(t) & -H_{21}^k(t) & -H_{21}^k(t) & -H_{22}^k(t) & 0 & H_{21}^k(t) \\ H_{12}^k(t) & 0 & 0 & 0 & -H_{11}^k(t) & 0 \\ 0 & -H_{22}^k(t) & H_{11}^k(t) & H_{12}^k(t) & -H_{21}^k(t) & -H_{11}^k(t) \end{pmatrix} \mathbf{A}^k(t), \tag{B7}$$

as a linear system of equations for the coefficients A_i^k from the ansatz, where we defined

$$\mathbf{A}^k(t) = (A_1^k(t), A_2^k(t), A_3^k(t), A_4^k(t), A_5^k(t))^T. \tag{B8}$$

The initial conditions for a time evolution operator in this notation are

$$\mathbf{A}^k(0) = (1, 0, 0, 0, 0)^T, \tag{B9}$$

where T denotes the transpose here (not the period of the time-dependent Hamiltonian). From here the time evolution operator was evaluated numerically.

Appendix C: Numerical calculation of time evolution operators using exact diagonalization

To study the J_1 - J_2 models in Eqs. (18), (22) and their approximate counterparts in Eqs. (31), (34) we employ exact diagonalization [90]. We note that the time evolution of a given initial state is more efficiently calculated using Krylov subspace methods, as in Ref. [55], and that DMRG-based methods are more powerful in the Floquet-MBL regime [91], being capable of reaching larger system sizes. Here we want, however, to compare the full time evolution operators using the most unbiased numerical method possible. To calculate this operator for a given (exact or approximate) Hamiltonian, we write

$$H(t) = H_0 + V(t), \quad (\text{C1})$$

where $V(t) \equiv 0$ for the time-independent effective Hamiltonians. We next ‘‘Trotterize’’ the problem by introducing discrete time steps $t_j = jT/N_{\text{steps}} \equiv j\delta t$, where δt is chosen small enough not to affect the results. Here T is the period of the time-dependent Hamiltonian. Then the time evolution operator over a period is given by

$$U(T, 0) = \prod_{j=0}^{N_{\text{steps}}-1} U(t_{j+1}, t_j), \quad (\text{C2})$$

where, using a second-order Trotter-Suzuki decomposition [92], we write

$$U(t + \delta t, t) = \exp\left[-\frac{i\delta t}{2\hbar}V\left(t + \frac{\delta t}{2}\right)\right] \exp[-i\delta t H_0/\hbar] \\ \times \exp\left[-\frac{i\delta t}{2\hbar}V\left(t + \frac{\delta t}{2}\right)\right]. \quad (\text{C3})$$

If the time dependence of $V(t)$ factors out, i.e. $V(t) = f(t)V_0$, the problem of calculating $U(T, 0)$ can be reduced to two matrix diagonalizations, of H_0 and V_0 , respectively, and numerically efficient matrix-matrix multiplications. If one of the matrices is integrable the problem can be simplified further, as in Ref. [36], but we do not assume that here. We write H_0 and $V(t)$ in a basis implementing translational invariance, and, for Eqs. (22), (34) also magnetization conservation [90]. The full diagonalization of the two matrices is achieved using the FEAST Eigenvalue Solver [93].

Appendix D: Transverse Ising model: BCH, Flow and replica Hamiltonians

In this section we summarize the treatment of the transverse Ising model.

1. Flow equations for the delta function model

The flow equations for the δ -function model, Eq.(38), in our approximation, Eq.(8), are found as

$$\begin{aligned} \frac{dC_x^{F,\delta}(s,t)}{ds} &= -h_x(\delta(t) - 1), \\ \frac{dC_z^{F,\delta}(s,t)}{ds} &= -h_z(\delta(t) - 1), \\ \frac{dC_{xx}^{F,\delta}(s,t)}{ds} &= -4h_z(t-1)C_{xy}^{F,\delta}(s,t), \\ \frac{dC_{xy}^{F,\delta}(s,t)}{ds} &= 2(t-1)[h_z(C_{xx}^{F,\delta}(s,t) - C_{yy}^{F,\delta}(s,t)) - h_x C_{xz}^{F,\delta}(s,t)], \\ \frac{dC_{yy}^{F,\delta}(s,t)}{ds} &= 4(t-1)[h_z C_{xy}^{F,\delta}(s,t) - h_x C_{yz}^{F,\delta}(s,t)], \\ \frac{dC_{xz}^{F,\delta}(s,t)}{ds} &= 2(t-1)[h_x C_{xy}^{F,\delta}(s,t) - h_z C_{yz}^{F,\delta}(s,t)], \\ \frac{dC_{yz}^{F,\delta}(s,t)}{ds} &= 2(t-1)[h_z C_{xz}^{F,\delta}(s,t) + h_x(C_{yy}^{F,\delta}(s,t) - C_{zz}^{F,\delta}(s,t))], \\ \frac{dC_{zz}^{F,\delta}(s,t)}{ds} &= 4h_x(t-1)C_{yz}^{F,\delta}(s,t), \end{aligned} \quad (\text{D1})$$

with initial conditions

$$\begin{aligned} C_x^{F,\delta}(0,t) &= h_x\delta(t), \\ C_z^{F,\delta}(0,t) &= h_z\delta(t), \\ C_{zz}^{F,\delta}(0,t) &= J_z, \\ C_{xx}^{F,\delta}(0,t) &= C_{xy}^{F,\delta}(0,t) = 0, \\ C_{yy}^{F,\delta}(0,t) &= C_{xz}^{F,\delta}(0,t) = C_{yz}^{F,\delta}(0,t) = 0. \end{aligned} \quad (\text{D2})$$

The solution at $s = 1$ gives coefficients

$$\begin{aligned} C_{x/z}^{F,\delta} &= h_{x/z}, \\ C_{xx}^F &= \frac{h_x^2 h_z^2 J_z (12h - 8\sin(2h) + \sin(4h))}{8h^5}, \\ C_{xy}^{F,\delta} &= \frac{h_x^2 h_z J_z \sin^4(h)}{h^4}, \\ C_{xz}^{F,\delta} &= \frac{h_x h_z J_z \left(h(2h_z^2 - h_x^2) + \sin(2h)(h_x^2 - h_z^2) - \frac{h_x^2 \sin(4h)}{4} \right)}{2h^5}, \\ C_{zz}^{F,\delta} &= \frac{J_z (4h(h_x^4 + 2h_z^4) + h_x^4 \sin(4h) + 8h_x^2 h_z^2 \sin(2h))}{8h^5}, \\ C_{yz}^{F,\delta} &= \frac{h_x J_z \sin^2(h) (h_x^2 \cos(2h) + h_x^2 + 2h_z^2)}{2h^4}, \\ C_{yy}^{F,\delta} &= -\frac{h_x^2 J_z (\sin(4h) - 4h)}{8h^3}, \\ C_{xzz}^{F,\delta} &= 0. \end{aligned} \quad (\text{D3})$$

2. Flow equations for the Heaviside θ -function model

The flow equations for the Heaviside θ -function model, Eq.(39), in our approximation, Eq.(8), are found to generate an infinite amount of terms. The terms that appear in Eq.(40) are generated quickly when using an ansatz that starts with the form of the original Hamiltonian, and subsequently adding the new terms that appear to that ansatz. This motivates one to include as many terms from the Hamiltonian Eq.(40) as possible while still allowing for a compact analytical result. We choose the ansatz Hamiltonian,

$$H_{\text{Ansatz}}^{F,\theta}(s) = \sum_i \left[C_x^{F,\theta} \sigma_i^x + C_z^{F,\theta} \sigma_i^z + C_{yy}^{F,\theta} \sigma_i^y \sigma_{i+1}^y + C_{zz}^{F,\theta} \sigma_i^z \sigma_{i+1}^z + C_{xz}^{F,\theta} (\sigma_i^x \sigma_{i-1}^z + \sigma_i^x \sigma_{i+1}^z) + C_{yz}^{F,\theta} (\sigma_i^y \sigma_{i-1}^z + \sigma_i^y \sigma_{i+1}^z) + C_{xzz}^{F,\theta} \sigma_i^x \sigma_{i-1}^z \sigma_{i+1}^z \right]. \quad (\text{D4})$$

The flow equations, Eq.(8), give us the following equations for the coefficients

$$\begin{aligned} \frac{dC_x^{F,\theta}(s,t)}{ds} &= -(4J_z C_{yz}^{F,\theta}(s,t) f_I(t) + h_x f(t)), \\ \frac{dC_z^{F,\theta}(s,t)}{ds} &= -h_z f(t), \\ \frac{dC_{yy}^{F,\theta}(s,t)}{ds} &= 4h_x C_{yz}^{F,\theta}(s,t) f_I(t), \\ \frac{dC_{xz}^{F,\theta}(s,t)}{ds} &= 2h_z C_{yz}^{F,\theta}(s,t) f_I(t), \\ \frac{dC_{yz}^{F,\theta}(s,t)}{ds} &= 2f_I(t) (J_z C_x^{F,\theta}(s,t) - h_z C_{xz}^{F,\theta}(s,t), \\ &\quad + J_z C_{xzz}^{F,\theta}(s,t) - h_x C_{yy}(s,t) + h_x C_{zz}(s,t)), \\ \frac{dC_{zz}^{F,\theta}(s,t)}{ds} &= (J_z f(t) - 4h_x C_{yz}^{F,\theta}(s,t) f_I(t)), \\ \frac{dC_{xzz}^{F,\theta}(s,t)}{ds} &= -4J_z C_{yz}^{F,\theta}(s,t) f_I(t), \end{aligned} \quad (\text{D5})$$

where $f(t) = \theta(t - \frac{1}{2})$, $f_I(t) = t + (1 - 2t)\theta(t - \frac{1}{2})$ and θ the Heaviside function. The initial conditions are

$$\begin{aligned} C_x^{F,\theta}(0,t) &= h_x (f(t) + 1), \\ C_z^{F,\theta}(0,t) &= h_z (f(t) + 1), \\ C_{zz}^{F,\theta}(0,t) &= -J_z (f(t) - 1), \\ C_{xx}^{F,\theta}(0,t) &= C_{xy}^{F,\theta}(0) = 0, \end{aligned} \quad (\text{D6})$$

$$C_{yy}^{F,\text{sgn}}(0,t) = C_{xz}^{F,\text{sgn}}(0,t) = C_{yz}^{F,\text{sgn}}(0,t) = 0.$$

The solution at $s = 1$ implies that the coefficients are

$$\begin{aligned} C_x^{F,\text{sgn}} &= h_x - \frac{4h_x J_z^2}{\gamma^2} \left(1 - \frac{\sin(\gamma)}{\gamma} \right), \\ C_z^{F,\text{sgn}} &= h_z, \\ C_{xx}^F &= C_{xy}^{F,\text{sgn}} = 0, \\ C_{xz}^{F,\text{sgn}} &= \frac{2h_x h_z J_z}{\gamma^2} \left(1 - \frac{\sin(\gamma)}{\gamma} \right), \\ C_{zz}^{F,\text{sgn}} &= J_z - \frac{4h_x^2 J_z}{\gamma^2} \left(1 - \frac{\sin(\gamma)}{\gamma} \right), \end{aligned} \quad (\text{D7})$$

where $\gamma = \sqrt{4h_x^2 + h_z^2 + 4J_z^2}$.

3. Result for the BCH identity

For the BCH identity one finds coefficients

$$\begin{aligned} C_x^{BCH} &= h_x, \\ C_z^{BCH} &= h_z, \\ C_{zz}^{BCH} &= J_z, \\ C_{yz}^{BCH} &= h_x J_z, \\ C_{xx}^{BCH} = C_{xy}^{BCH} = C_{xz}^{BCH} = C_{yy}^{BCH} = C_{xzz}^{BCH} &= 0. \end{aligned} \quad (\text{D8})$$

4. Result for the replica approximation

The coefficients for the replica case were taken from Ref.[88] as

$$\begin{aligned} C_x^R &= h_x \left(J_z \cot(2J_z) + \frac{1}{2} \right), \\ C_z^R &= h_z, \\ C_{zz}^R &= J_z, \\ C_{yz}^R &= \frac{1}{2} h_x J_z, \\ C_{xzz}^R &= h_x \left(J_z \cot(2J_z) - \frac{1}{2} \right), \\ C_{xx}^R = C_{xy}^R = C_{xz}^R = C_{yy}^R &= 0. \end{aligned} \quad (\text{D9})$$